ARTHROPOD SYSTEMATICS & PHYLOGENY

76 (3): 429–447
11.12.2018

SENCKENBERG

On the verge of below-ground speciation: a new species complex of microendemic endogean carabid beetles, *Typhlocharis* Dieck, 1869 (Coleoptera: Carabidae: Anillini), from south-west Iberian Peninsula

Sergio Pérez-González*[,1], Carmelo Andújar[2], Esther Lantero[3] & Juan P. Zaballos[1]

[1] Departamento de Biodiversidad, Ecología y Evolución, Unidad Docente de de Zoología y Antropología Física, Facultad de Ciencias Biológicas, Universidad Complutense de Madrid, 28040, Spain; Sergio Pérez-González * [seper01@ucm.es]; Juan P. Zaballos [zaballos@ucm.es] — [2] Grupo de Ecología y Evolución en Islas, Instituto de Productos Naturales y Agrobiología (IPNA-CSIC), San Cristóbal de la Laguna, 38206, Spain; Carmelo Andújar [candujar@um.es] — [3] Departamento de Genética, Fisiología, y Microbiología, Unidad Docente de Genética, Facultad de Ciencias Biológicas, Universidad Complutense de Madrid, 28040, Spain; Esther Lantero [estherlantero@ucm.es] — * Corresponding author

Accepted 24.iv.2018.
Published online at www.senckenberg.de/arthropod-systematics on 27.xi.2018.
Editors in charge: Julia Goldberg & Klaus-Dieter Klass

Abstract. A new species complex of genus *Typhlocharis* Dieck, 1869 (Coleoptera: Carabidae: Trechinae: Anillini: Typhlocharina) is described. Six populations from southern Badajoz (Spain), referred as the "*coenobita* species complex", are the first documented case of an expected situation within Typhlocharina and potentially other lineages of endogean ground beetles: the presence of closely related allopatric populations within a reduced geographical range that, despite certain genetic isolation, show a gradient of morphological differences that challenge taxonomic assignment. Previous phylogenies of Typhlocharina recovered these populations as a monophyletic lineage, represented by three potential new species in need of further examination to validate their status. Here, we test the congruence of this taxonomic hypothesis through direct observation, statistical analyses applied to morphological characters and analysis of COI sequences. Such integrative approach, revealed as a powerful tool to solve situations where phenotypic differences are very subtle, is used for the first time to discriminate Anillini species. The results are coherent with the three species hypothesis, formally described as *T. coenobita* **sp.n.**, *T. eremita* **sp.n.** and *T. anachoreta* **sp.n.** The implications of the internal variability within this species complex to the systematics of Typhlocharina and their affinities to other *Typhlocharis* species are discussed. The entity of *T. eremita* **sp.n.** as new species is well established within the standards of the genus. However, the populations of *T. coenobita* **sp.n.** show high variability and their relationship with *T. anachoreta* **sp.n.** is in the verge of what can be considered species-level differentiation, suggestive of an incipient speciation process. The proposed species boundaries maximize the consistence among the different sources of evidence. The intraspecific variability within *T. coenobita* **sp.n.** is properly described, contributing to elucidate the ongoing differentiation processes within this endogean lineage. Finally, an identification key for the *coenobita* species complex is provided.

Key words. Endogean, Coleoptera, Carabidae, *Typhlocharis*, taxonomy, new species, speciation, systematics, species complex.

1. Introduction

"*Given any species in any region, the related species is not likely to be found in the same region*" (Jordan 1905: p. 547).

The evolution of genetic reproductive barriers between geographically separated populations (allopatric speciation, Mayr 1963) has been widely accepted as a prevalent mode of speciation in animals (Futuyma 1998; Coyne & Orr 2004). The initial geographical separation may be due to the emergence of an extrinsic barrier, extinction of intervening population, or migration into a separate region (Futuyma 1998; Coyne & Orr 2004; Lomolino

et al. 2010). Indeed, dispersion through a heterogeneous geography or landscape has the potential to generate geographically isolated populations that become the source for the speciation process. In species that disperse little or are strongly tied to a particular habitat, spatial scale of speciation can be strongly reduced and barriers to gene flow may isolate populations at a microgeographic scale (Futuyma 1998; Kisel & Barraclough 2010).

Both conditions are generally met by species adapted to live in deep soil layers, and particularly by the subtribe Typhlocharina Jeanne, 1973 (Coleoptera: Carabidae: Trechinae: Anillini). This endogean lineage of carabid beetles is endemic to some areas of the western Mediterranean region, distributed through the Iberian Peninsula (Spain and Portugal) and the north of Africa (Morocco and Tunisia) (Zaballos 2003). A strong pattern of geographical speciation has been shown in Typhlocharina (Jeannel 1963; Andújar et al. 2016, 2017), becoming the most diversified group of Anillini known up to date. These animals are specialists of the endogean environments, inhabiting the soil horizons A and B (Ortuño 2000). Thus, they are morphologically well suited to the specific conditions below soil: eyeless, wingless, depigmented, with short limbs, narrow, rectangular bodies and tiny sizes (0.9–2.9 mm). Within Anillini, they are easily recognizable by the square-shaped pronotum and the unusual female genitalia (Vigna-Taglianti 1972; Zaballos & Wrase 1998; Pérez-González & Zaballos 2012).

Currently, given the unprecedented and increasing rate of new species descriptions, the study of the group is going through one of its most complex moments (Zaballos et al. 2016; Serrano & Aguiar 2017). The first approach to the systematics of Typhlocharina established species groups based on key morphological features, with special emphasis in the umbilicate series of setal insertions (Zaballos & Ruíz-Tapiador 1997; Zaballos & Wrase 1998; Pérez-González & Zaballos 2013c). Notwithstanding, recent efforts to resolve the phylogeny of Typhlocharina based on morphological, molecular and total evidence data (Pérez-González et al. 2017; Andújar et al. 2017) showed that these species groups do not correlate with true clades and concluded in the subdivision of the former genus *Typhlocharis* Dieck, 1869 in three different genera: *Lusotyphlus* Pérez-González, Andújar & Zaballos, 2017; *Typhlocharis* Dieck, 1869 and *Microcharidius* Coiffait, 1969 (Pérez-González et al. 2017). As a consequence of the sampling efforts towards the phylogeny of the group, many new populations were discovered, which may represent more than 45 potential new species yet to be formally corroborated and described (Pérez-González et al. 2017; Andújar et al. 2017).

Now, the case of six closely related populations of *Typhlocharis* found in a small area of about 60 × 60 km in south-west Iberian Peninsula is presented. These populations were recovered as a well-supported monophyletic lineage represented by three potential species with clear morphological affinities (named "*T.* sp. 6", "*T.* sp. 7" and "*T.* sp. 8" in Pérez-González et al. 2017 and Andújar et al. 2017).

However, "species delimitation" is not an easy task and these potential "new species" need further examination to validate their status and provide a formal description. Cases of intraspecific phenotypic variation that challenge the identification criteria for species-level taxa in Typhlocharina have been recently evidenced, as recorded for *Typhlocharis singularis* Serrano & Aguiar, 2000; *T. mixta* Pérez-González, Zaballos & Ghannem, 2013 and *Microcharidius zaballosi* Serrano & Aguiar, 2014 (Serrano & Aguiar 2000, 2002, 2014; Pérez-González et al. 2013). The problem of species discrimination is widely extended in zoology (e.g. De Queiroz 2007; Willis 2017; Andújar et al. 2014) and the frontiers between intra- and interpopulation variability and speciation are diffuse at the scale of microevolutionary changes. Here, we test the congruence of morphological and molecular data with the hypothesis of the six studied populations as three different species. The new species are described and their relationships and limits are discussed, as well as the implications of microevolutionary changes and intrapopulation variability for the systematics of the genus, which would help to understand population dynamics and speciation in endogean environments.

2. Material and methods

2.1. Collecting

The study area occupies a range of about 60 × 60 km, located in the south of Badajoz province (Spain). Soil samples were collected in winters 2012 and 2013 from six localities (Figs. 1, 2): Valverde de Leganés (VL); Almendral, Ribera La Albuera (LA); Higuera de Vargas (HV); Aceuchal, Río Guadajira (RG); Valverde de Burguillos (VB) and Oliva de la Frontera, Arroyo Zaos (AZ). Samples included superficial and deep soil layers (horizons A and B) up to 30–50 cm deep and were processed in the field using an optimized version of the soil washing technique (Normand 1911). The fauna was extracted from the samples with Berlese apparatus (Berlese 1905). In some sites, additional specimens were collected by hand, under deeply buried boulders of several sizes, using a thin (nº 000) white haired paintbrush. Overall, 1020 specimens were collected and stored in absolute ethanol.

2.2. Morphological study

For the morphological observations, specimens were rinsed in lactic acid to clear the cuticle. A minimum of five males and five females of each population (except for VL population, where only three specimens were available) were dissected by separation of the body parts and extraction of the male genitalia for a detailed observation of the structures. Female genitalia were studied *in situ*, by transparence, to avoid the damage of delicate

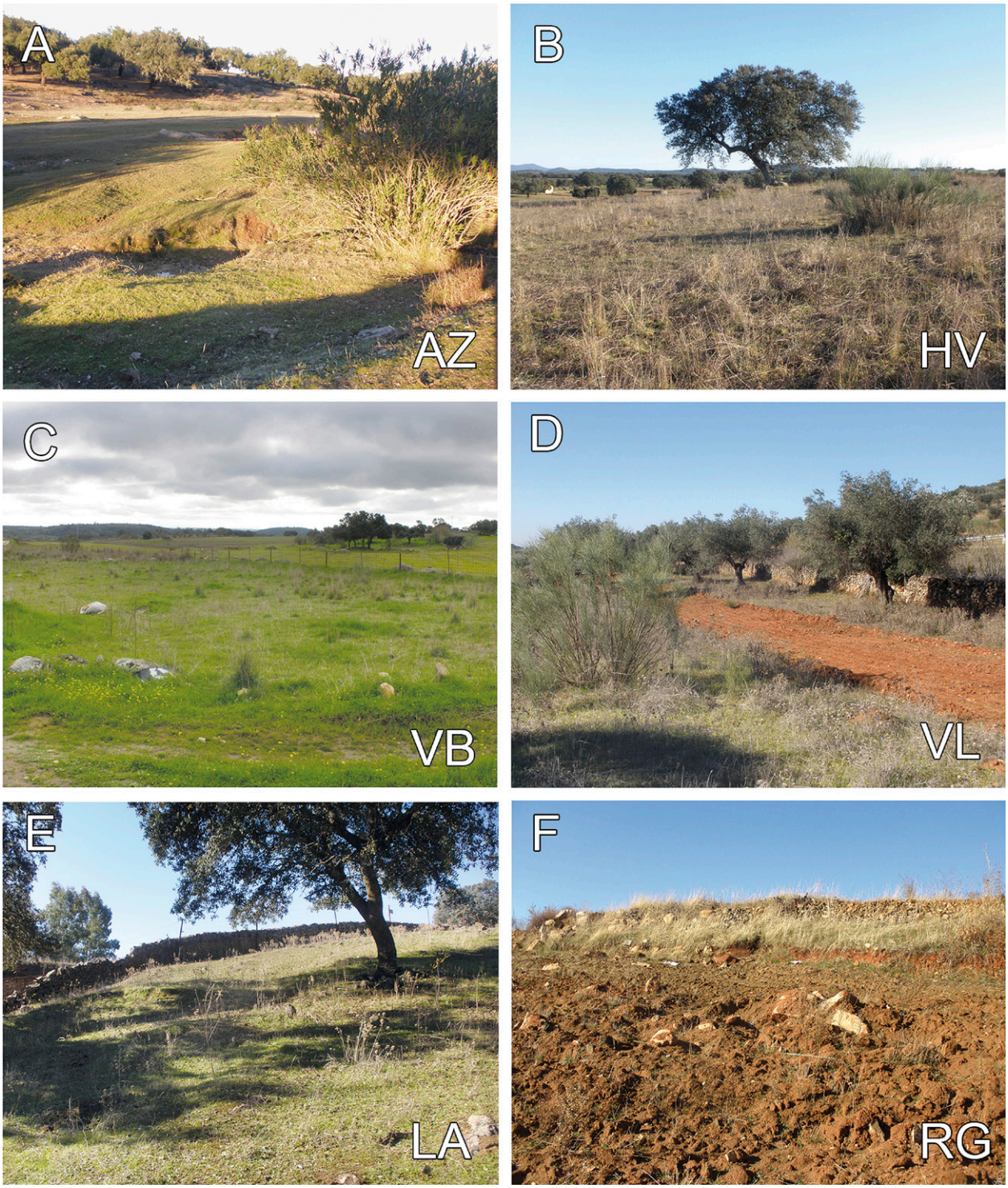

Fig. 1. Sampled localities (south of Badajoz province, Spain). **A**: Small slope of a temporary watercourse in an alluvial plain in Arroyo Zaos, 2.8 km N Oliva de la Frontera (AZ); **B**: open grassland and thistle pasture field 3.15 km S of Higuera de Vargas (HV); **C**: meadow surrounded by cultures and open holm oak forest 4.4 km N of Valverde de Burguillos (VB); **D**: olive tree culture 1.9 km SE of Valverde de Leganés (VL); **E**: pasture land near a small river, Ribera La Albuera, 1.5 km NW Almendral (LA); **F**: open culture and grassland area near Río Guadajira, 2.7 km SW Aceuchal (RG).

structures during manipulation. There are 44 specimens with a voucher number, selected for DNA extraction (detailed in Pérez-González et al. 2017 and Andújar et al. 2017) that were also observed in detail, but dissection were restricted to the extraction of male genitalia. The remaining specimens of each population were kept intact but observed and compared to dissected specimens to ensure the identification.

All the observations were made using light microscopy. The nomenclature used follows Zaballos (2005) for cephalic chaetotaxy, Pérez-González & Zaballos (2012, 2013c) for the rows of setae and Pérez-González

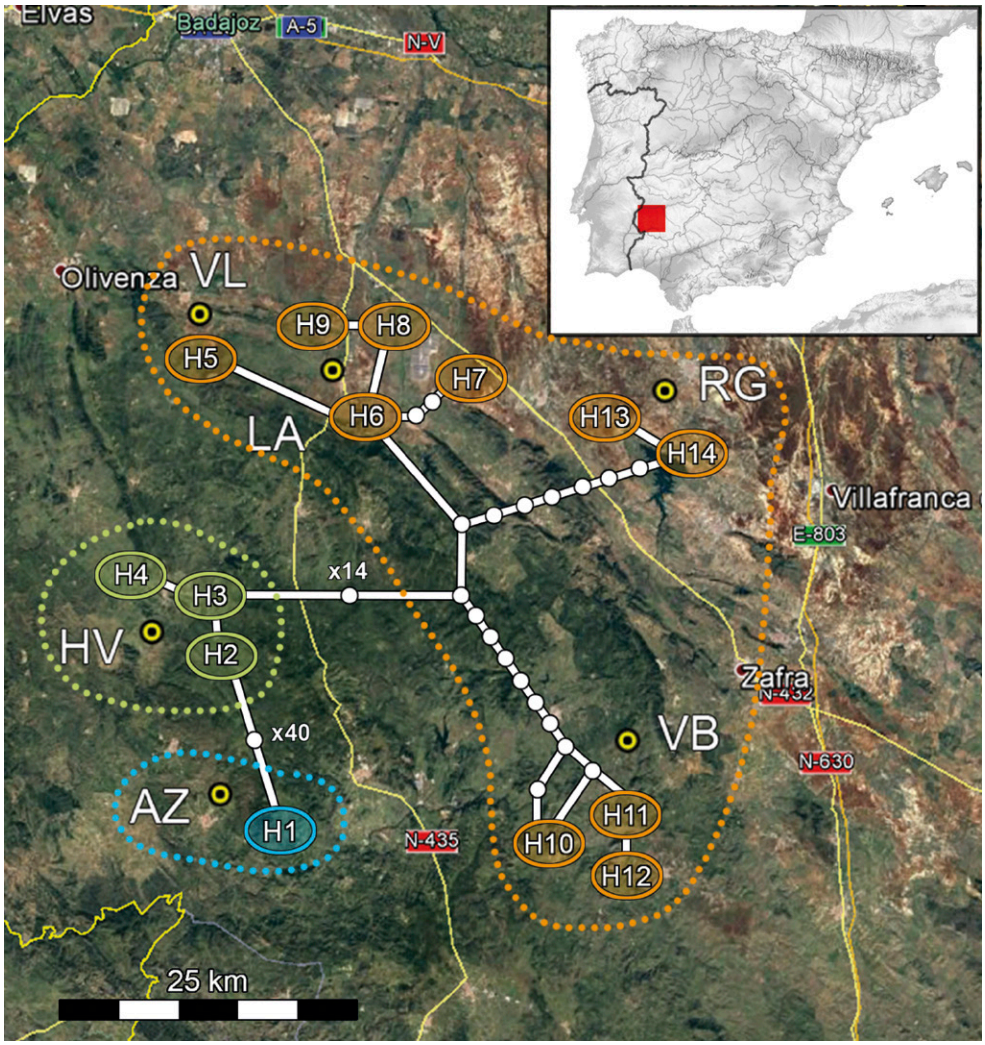

Fig. 2. Map of the distribution range of the six studied populations including the TCS Haplotype network from the COI sequences of 34 specimens. Localities named as in Fig. 1. Haplotypes named as in Table S1.1, size of the labels is not proportional to the number of specimens in each haplotype.

& Zaballos (2013b) for antennal features. Terminology for the IX sclerite of males follows Sokolov & Kavanaugh (2014). Measurements were made with a Wild Heerbrugg M8 stereomicroscope (Switzerland). Drawings were made from photographs obtained using a Zeiss 474620-9900 microscope (Germany), processed and outlined with Adobe Photoshop CS6 13.0.

After the observations, dissected specimens and extracted genitalia were mounted on entomological cards with glass window using dimethyl hydantoin formaldehyde resin (Bameul 1990). Untreated specimens were mounted on regular entomological cards. Specimens with voucher number (El. Suppl. File 1 Appendix S1: Table S1.1) were fluid-preserved in Eppendorfs with absolute ethanol. The type specimens are deposited in Coll. J.P. Zaballos and Coll. S. Pérez-González, Universidad Complutense de Madrid (UCM, Madrid), Natural History Museum (NHM, London) and Museo Nacional de Ciencias Naturales (MNCN, Madrid).

The morphological matrix used in Pérez-González et al. (2017) was adapted to code those morphological features that showed variation between the studied populations (Table 1) in the 44 voucher specimens (8 from AZ, 8 from HV, 8 from VB, 8 from LA, 2 from VL, 10 from RG). Character states within some traits (e.g. ring sclerite) were re-coded to register additional variations at population level. Characters were coded as binary or multistate if they can be considered part of a transition (e.g. degree of development of lateral denticles of elytra). Multistate characters that could not be considered ordered (ring sclerite) were split as several binary dummy variables, one for each character state, generating a final set of 23 characters (El. Suppl. File 1 Appendix S1: Table S1.2). Two matrixes were produced, one at specimen level (vouchered individuals, 44 terminals) and one at population level (6 terminals) (El. Suppl. File 1 Appendix S1: Tables S1.3, S1.4).

UPGMA analyses were conducted on both matrixes to cluster the terminals by morphological similarity using DendroUPGMA online facility (http://genomes.urv.cat/UPGMA/), assuming Euclidean distances and applying bootstrap with 100 replications (El. Suppl. File 2 Appendix S2).

The hypothesis of three species for these populations (Pérez-González et al. 2017; Andújar et al. 2017) was tested through discriminant analysis using STATGRAPHICS Centurion XVII (StatPoint, Inc., USA, 2014), applied to the individual level matrix excluding non-informative characters (El. Suppl. File 2 Appendix S3). This analysis distinguishes between groups in a given dataset, generating a series of discriminant functions based on the observed variables (the morphological characters). The 44 cases of the matrix were used to develop a model to discriminate among the three proposed groups ("species": "A" for "*T.* sp. 8", "B" for "*T.* sp. 7" and "C" for "*T.* sp. 6"), using stepwise regression (backward selection) to determine which variables are significant predictors. The obtained discriminant functions can be used to classify new observations in one of the three groups. To test the performance of the classification function coefficients, 43 specimens were additionally coded and analyzed: 5 males and 5 females from VB, RG, LA and HV respectively, and 3 females of AZ. Due to lack of extra specimens, VL was not included. Data matrix of the 43 additional specimens, table of classification function coefficients, functions used to classify observations and results of the predictions are given in El. Suppl. File 1 Appendix S1: Table S1.5; El. Suppl. File 2 Appendix S3: Table S3.1.

The results are discussed within the phylogenetic framework of Typhlocharina proposed in Pérez-González et al. (2017) and Andújar et al. (2017).

2.3. Molecular study

Genetic differentiation between populations was inferred using sequences of the barcoding region of the Cytochrome Oxidase Subunit I (COI) gene, available for 34 of the 44 vouchered specimens (Genbank accession numbers in El. Suppl. File 1 Appendix S1: Table S1.1; from Andújar et al. 2017). DNA was aligned using MAFFT G-INS-I algorithm (Katoh et al. 2002) and trimmed to a final dataset of 657 bp in Geneious 7.1.9 (Kearse et al. 2012). Phylogenetic maximum likelihood inferences were done with IQTree 1.5.5 (Nguyen et al. 2015). The best fitting model of evolution was estimated with ModelFinder (Kalyaanamoorthy et al. 2017) and nodal support was obtained by 1000 ultrafast bootstrap (UFBoot) replicates (Minh et al. 2013).

The software TCS (Clement et al. 2000) was used to estimate an haplotype network based on Statistical Parsimony (Templeton et al. 1992) using the 34 COI sequences and a dataset trimmed to 523 bp. K2p distances (Kimura 1980) were calculated with MEGA version 5 (Tamura et al. 2011) and were visualized on a principal coordinates plot (PCoA) using NTSYSpc v.2.10q software (Rohlf 2000). To assess structuring within and among the populations, Analyses of Molecular Variance (AMOVA) were carried out in Arlequin v.3.5.1.2 (Excoffier & Lischer 2010) with 1000 permutations (El. Suppl. File 2 Appendix S4).

3. Results

3.1. Morphological variation between populations

The studied specimens from VB, VL, LA, RG, HV and AZ belong to genus *Typhlocharis* (*sensu* Pérez-González et al. 2017), defined by the shape of last ventrite, with a smoothly curved posterior margin and presence of abdominal belt. These populations are very akin to each other and are characterized within *Typhlocharis* by the combination of several morphological features (Table 1). All of them share the presence of two terebral teeth, a row of setae in the anterior margin of pronotum with a trend to alternate lengths, umbilicate series with 4+3 or 4+2 patterns, elytral apex without denticles and a characteristically projected apex of the ring sclerite of the male genitalia, with diverse types of "spoon-like" shapes.

The observed range of intrapopulation variability is similar to that described for other species of *Typhlocharis*, such as *T. mixta* or *T. mendesi* Serrano & Aguiar, 2017 (Pérez-González et al. 2013; Serrano & Aguiar 2017). The labrum, mandibles, pronotum, transverse scutellar organ, elytral buttonholes or the elytral apex shape are prone to minor variations between individuals, as well as body size and degree of sclerotization. Individual variability is also common on the patterns of chaetotaxy in labium, basilar, sensilla coeloconica (**sc**) of the last antennomere, anterior and posterior rows of pronotum or last ventrite.

The main morphological traits that differ among populations are detailed in Table 1. It is noteworthy that the majority of differentiating characters are not discrete, but part of a morphological spectrum and frequently overlaps between populations. For example, the median lobe of the ligula is especially prominent and notorious in the population of HV (Table 1), yet in the other populations, some individuals show very prominent median lobes of ligula that approach to the less developed shapes seen in HV population. For this reason, differentiation between species should not rely on one specific character, but a combination of several features.

UPGMA analyses based on these morphological characters clustered the populations as shown in Fig. 3. The results from the "population level" matrix and the "specimen level" matrix were consistent (El. Suppl. File 2 Appendix S2: Tables S2.1, S2.2 and Figs. S2.1, S2.2), despite general low support. Both analyses recovered a low supported topology with AZ and HV as well differentiated entities and the remaining populations as part of the same cluster. Within this cluster, LA, VL and VB were recovered close to each other and RG more distant. This topology, even if non-supported, is consistent with the proposed hypothesis of three species, corresponding to "species A" - LA+VL+VB+RG, "species B" - HV and "species C" - AZ (Fig. 3).

Results of the discriminant analysis over the 44 voucher specimens also supported the same classifica-

Table 1. Comparison of the morphological features that show differences among the studied populations of *Typhlocharis* from south west Iberian Peninsula. — ***Abbreviations***: **AZ**, Oliva de la Frontera, Arroyo Zaos; **HV**, Higuera de Vargas; **VL**, Valverde de Leganés; **LA**, Almendral, Ribera La Albuera; **VB**, Valverde de Burguillos, **RG**, Aceuchal, Río Guadajira.

Population	Total length (mm)	Left mandible	Right mandible	Median lobe of ligula	Labrum	Semilunar notch	Shape of pronotum	Medial hiatus	Crenulation of anterior margin	Posterolateral denticles of pronotum
AZ	1.26–1.43	Inner edge subtly projected (smooth flap)	Two terebral teeth	Curved and prominent (shorter than paraglossae)	Subquadrate or rounded	Faint	Subquadratre or subrectangular	2–2.5 spaces	Well marked	3–5, strong, well defined
HV	1.17–1.45	Inner edge subtly projected (smooth flap)	Two terebral teeth	Very prominent (as long or longer than paraglossae)	Subquadrate or rounded	Well marked	Subquadratre	3 spaces	Moderately marked	3–5, well defined, irregular
VL	1.24–1.27	Inner edge subtly projected (smooth flap)	Two terebral teeth	Curved and prominent (shorter than paraglossae)	Rounded	Well marked	Subquadratre	1.5–2 spaces	Slightly marked	2–3, low and blunt
LA	1.12–1.27	Inner edge subtly projected (smooth flap)	Two terebral teeth, the second with individual variation	Curved and prominent (shorter than paraglossae)	Subquadrate or rounded	Well marked	Subquadratre	1.5–2 spaces	Slightly marked	2–4, low and blunt
VB	1.11–1.40	Smooth inner edge	Two terebral teeth, the second with individual variation	Curved and prominent (shorter than paraglossae)	Subquadrate or rounded	Well marked	Subquadratre	1.5–2 spaces	Moderately marked	2–3, low and blunt
RG	1.13–1.27	Inner edge subtly projected (smooth flap)	Two terebral teeth, the second with individual variation	Prominent, but shorter than paraglossae	Subquadrate	Well marked	Subquadratre	2.5–3 spaces	Slightly marked	2–4, blunt and irregular

Population	Transverse scutellar organ	Shape of elytral ápex	Lateral denticles of elytra	Umbilicate series	Subapical / Apical setae of elytra	Shape of metafemora	Inner margin of femora	Endophallic sclerites	Distal expansion of ring sclerite	Shape of spermatheca
AZ	Variable, straight or smoothly curved	"v-shaped" notch	Moderately marked	4+2	Row of short setae, apical pair not longer than the rest	Normal	Smooth	rod-shaped, arranged in a "branched" structure	subtriangular	Subsphaeric (predominant) or ovoid
HV	Variable, from straight to strongly subtriangular	Round	Strongly marked, defined in last third	4+3	Row of long, thin setae, apical pair slightly longer than the rest	Angular	Smooth	forked, with a curved lateral projection pointing upwards	"spoon-shaped", variable, usually more or less square	Subsphaeric (predominant) or ovoid
VL	Variable, tipically smoothly subtriangular	Round	Very faint	4+2	Row of long, thin setae, apical pair variable, usually slightly longer than the rest	Normal or slighty angular	Smooth	forked, with a curved lateral projection pointing upwards	? (males unknown)	Ovoid (predominant) or subsphaeric
LA	Variable, tipically smoothly subtriangular	Round	Very faint	4+2	Row of long, thin setae, apical pair variable, usually slightly longer than the rest	Normal or slighty angular	Smooth	forked, with a curved lateral projection pointing upwards	"spoon-shaped", variable	Ovoid (predominant) or subsphaeric
VB	Variable, tipically curved or smoothly subtriangular	Round or smoothly notched	Faint	4+2	Row of long, thin setae, apical pair not longer than the rest	Angular	Coarse or smooth	forked, with a curved lateral projection pointing upwards	"spoon-shaped", rounded	Subsphaeric, rarely ovoid
RG	Subtriangular	Round	Faint	4+3	Row of long, thin setae, apical pair variable, usually slightly longer than the rest	Angular	Smooth	rod-shaped, forked, with a curved lateral projection pointing upwards	"spoon-shaped", variable, usually more or less square	Subsphaeric

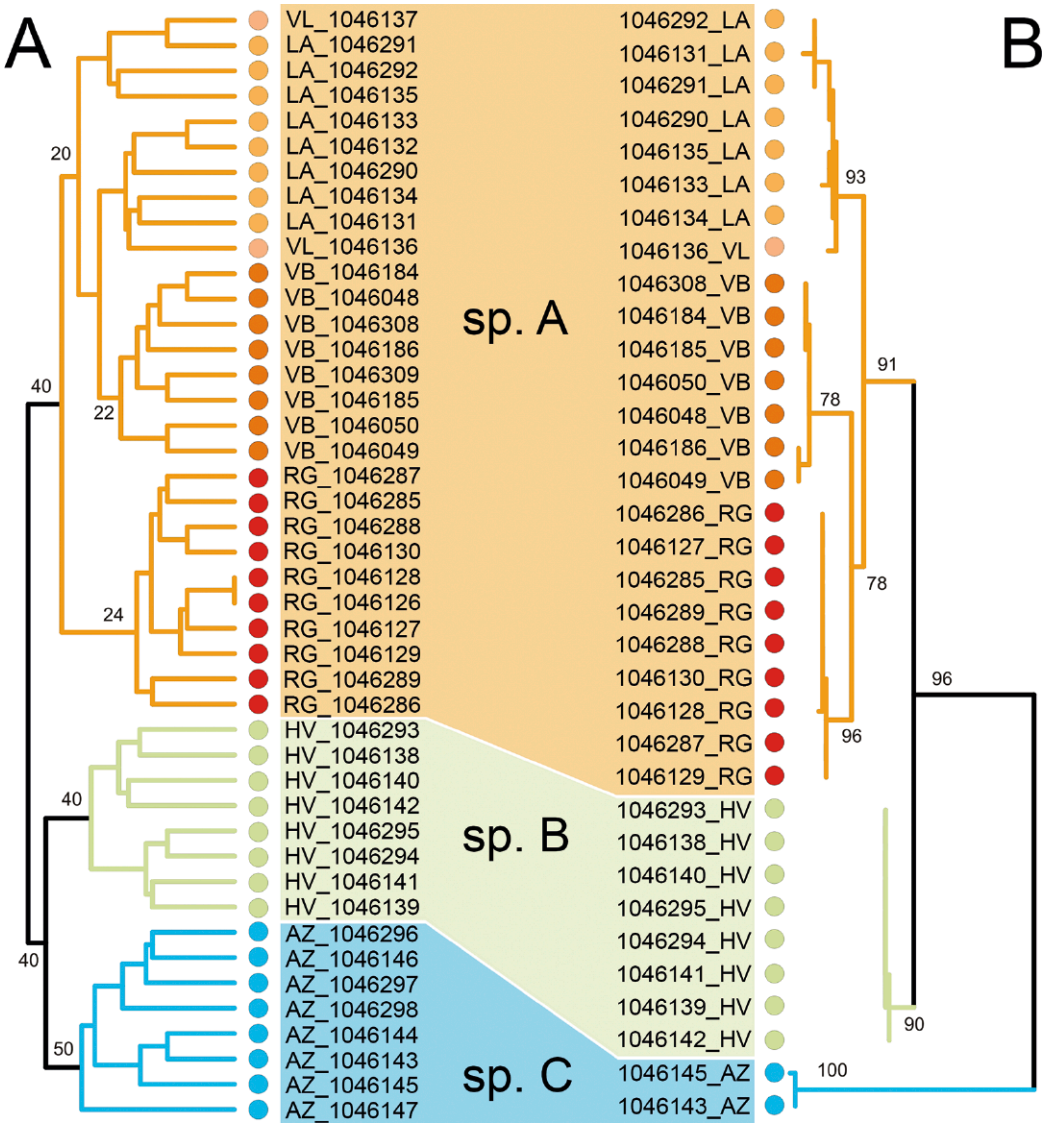

Fig. 3. Hypothesis of three species within the six studied populations contrasted to morphological and molecular evidences (species A, B and C equivalent to "*T.* sp. 8"; "*T.* sp. 7" and "*T.* sp. 6" respectively, from Pérez-González et al. 2017). **A**: "Specimen-level" UPGMA dendrogram clustering the 44 vouchered specimens by morphological similarity according to 23 characters. **B**: ML tree from the COI sequences of 34 specimens. Numbers at each node represent bootstrap values (over 100).

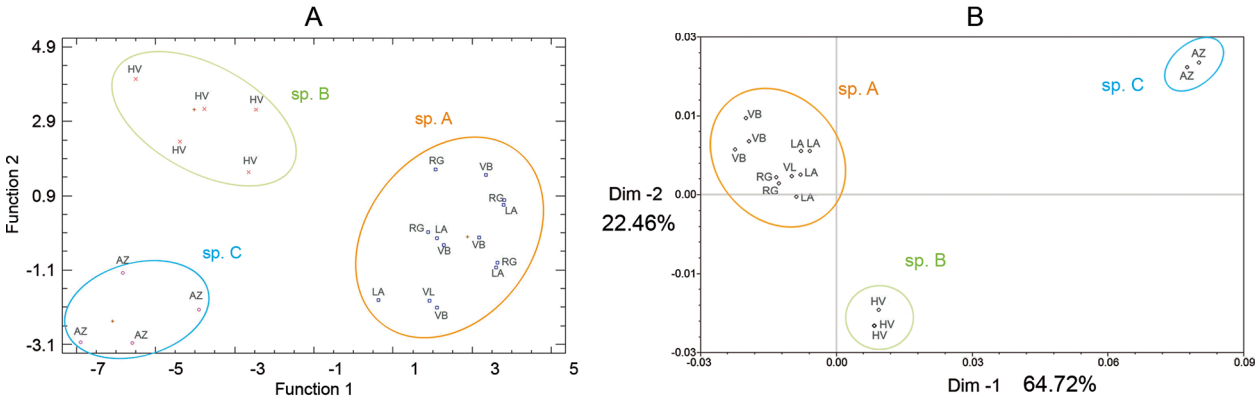

Fig. 4. A: Discriminant Analysis based on morphological characters. **B**: Principal Component Analysis based on the k2p distances.

tion (Fig. 4A). Six characters (median lobe of ligula, posterolateral denticles of pronotum, shape of elytral apex, lateral denticles of elytra, pattern of umbilicate series and shape of metafemora) were effective altogether to recognize the proposed three species and correctly classify **100%** of the cases (El. Suppl. File 2 Appendix S3).

The 43 additional specimens used to test the classification were also recovered in the expected groups in all the cases (El. Suppl. File 2 Appendix S3: Table S3.1).

3.2. Analyses of genetic differentiation

As a preliminary approach trying to figure out if the morphological data were supported by the available molecular data, the 34 DNA sequences from the studied populations were used to assess the genetic structure within this *Typhlocharis* complex.

The maximum likelihood tree obtained in IQTree for the COI dataset shows clades well supported as monophyletic grouping specimens from individual localities (with VL and LA together) and is fully congruent with the hypothesis of three species (Fig. 3). Specimens from "species C" - AZ are supported as monophyletic (Bootstrap support = bs 100) and are sister to the lineage with the remaining specimens. This lineage is divided in two main clades, one including all specimens from "species B" - HV (bs 96) and the other, "species A" - LA+VL+VB+RG (bs 91), including all the remaining populations. Within the latter, there are three clades corresponding to specimens from RG (bs 96), VB (bs 78) and LA+VL (bs 93) respectively, with RG and VB (bs 78) well supported as monophyletic (Fig. 3).

The 34 COI sequences, after trimming to 523 bp, defined 14 haplotypes, none of them shared among populations. The parsimony haplotype network from TCS (Fig. 2) showed how haplotypes from HV (named H2, H3 and H4) diverge from haplotype H1 (characteristic from AZ) by 40 mutational steps supporting the differentiation of these two groups. HV is separated by at least 17 mutational steps from the closest haplotype (H6) within the third group, which included haplotypes from VB, RG, LA and VL. Among the latter populations, the distance between VB and VL is 11 mutational steps, between RG and VL is 8 and between VB and RG is 17.

AMOVA results grouping populations according to the three species hypothesis revealed that 2/3 of the genetic variance were due to the differences among groups. Also, these three genetic groups seemed to be heterogeneous given that 27.8% of the genetic variance was caused by differences among population within groups (El. Suppl. File 2 Appendix S4). This genetic structure was supported by K2P distances among the 14 haplotypes detected in the sample. These distances were visualized on a PCoA (Fig. 4B) where the x-axis split the haplotypes in the same three groups defined by the morphological characters.

These results must be taken with caution, since there are very few individuals from each population with available molecular data. However, this preliminary approach is largely congruent with the observed morphological differences and both approaches are consistent with the initial hypothesis. Hence, we propose that the six studied populations are part of a complex within genus *Typhlocharis* represented by three different species.

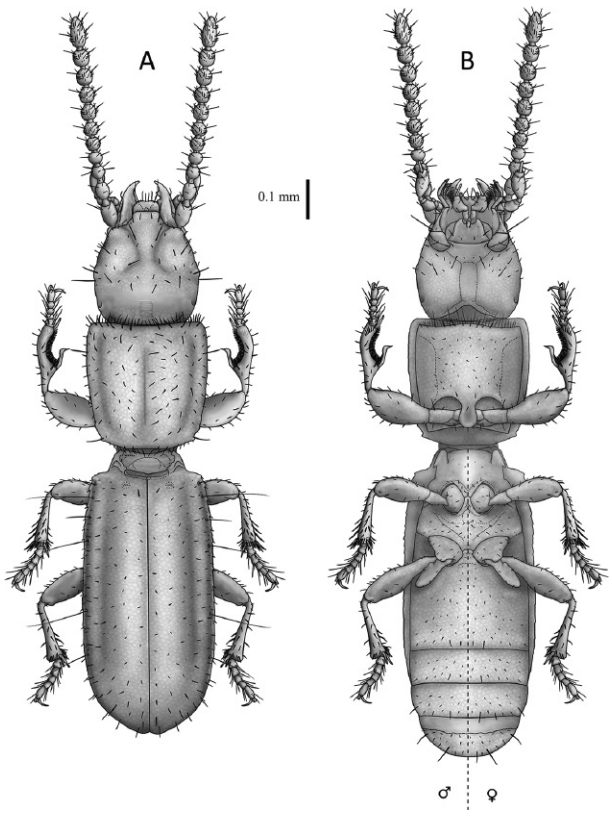

Fig. 5. *Typhlocharis coenobita* sp.n. **A**: Habitus, dorsal view (male); **B**: habitus, ventral view (abdominal morphology: left half, male; right half, female).

3.3. Description of species

***Typhlocharis coenobita* sp.n.**

Locus typicus. Valverde de Burguillos, Badajoz, España.

Material examined. ***Type series***: Holotype: 1 ♂ SPAIN, Badajoz, Valverde de Burguillos, Ctra EX-101, km 18, (38°21′N 06°31′W), 22.xi.2012, 488 m, J.P. Zaballos, S. Pérez-González & S. Ghannem leg. (Coll. J.P. Zaballos, UCM). – Paratypes: 176 ♂♂, 183 ♀♀ same data as the holotype (Coll. J.P. Zaballos and Coll. S. Pérez-González, UCM), 2 ♂♂, 2 ♀♀ same data as the holotype (MNCN), 4 ♂♂ (BMNH-1046048, BMNH-1046049, BMNH-1046050, BMNH-1046184), 4 ♀♀ (BMNH-1046185, BMNH-1046186, BMNH-1046308, BMNH-1046309) same data as the holotype (Coll. C. Andújar, NHM, Coll. J.P. Zaballos and Coll. S. Pérez-González, UCM). DNA aliquots deposited in NHM, London (voucher nº BMNH-1046048, BMNH-1046049, BMNH-1046050, BMNH-1046184, BMNH-1046185, BMNH-1046186, BMNH-1046308 and BMNH-1046309). — ***Other specimens***: 20 ♂♂, 9 ♀♀, 1 ? SPAIN, Badajoz, Almendral (1.5 km NW), Ribera La Albuera (38°37′N 06°49′W), 3.xii.2013, 309 m, J.P. Zaballos & S. Pérez-González leg. (Coll. J.P. Zaballos and Coll. S. Pérez-González, UCM), 5 ♂♂ (BMNH-1046290, BMNH-1046291, BMNH-1046131, BMNH-1046132, BMNH-1046133), 3 ♀♀ (BMNH-1046292, BMNH-1046134, BMNH-1046135) same data (Coll. C. Andújar, NHM, Coll. J.P. Zaballos and Coll. S. Pérez-González, UCM). 1 ♀ SPAIN, Badajoz, Valverde de Leganés (1.9 km SE) (38°39′N 06°57′W), 3.xii.2013, 377 m, J.P. Zaballos & S. Pérez-González leg. (Coll. J.P. Zaballos, UCM), 2 ♀♀ (BMNH-1046136, BMNH-1046137) same data (Coll. C. Andújar, NHM, Coll. J.P.

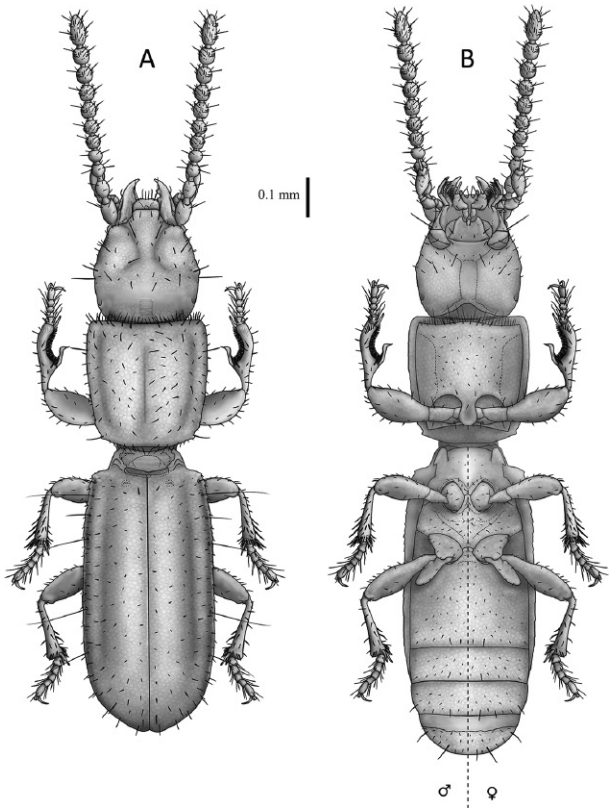

Fig. 6. *Typhlocharis eremita* sp.n. **A**: Habitus, dorsal view (male); **B**: habitus, ventral view (abdominal morphology: left half, male; right half, female).

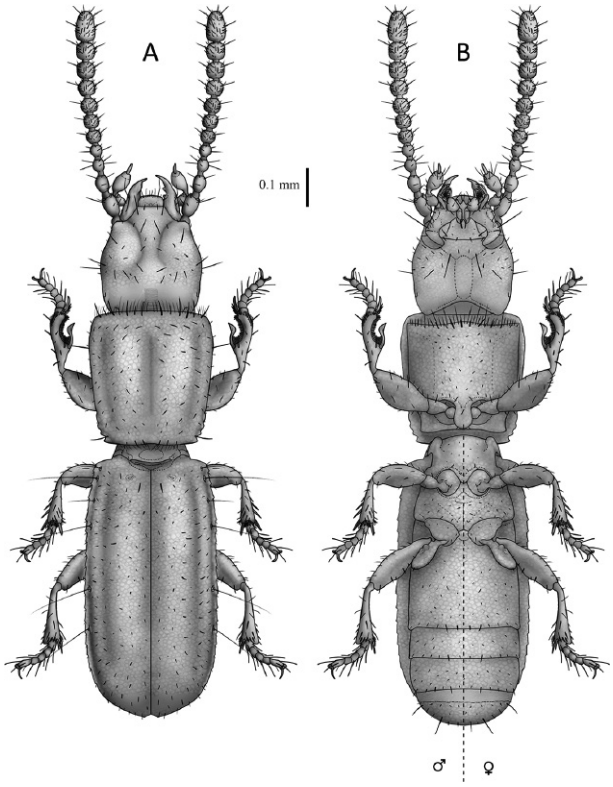

Fig. 7. *Typhlocharis anachoreta* sp.n. **A**: Habitus, dorsal view (male); **B**: habitus, ventral view (abdominal morphology: left half, male; right half, female).

Zaballos, UCM). 27 ♂♂, 17 ♀♀, 2 ? SPAIN, Badajoz, Aceuchal (2.7 km SW), Río Guadajira (38°37′N 06°30′W), 3.xii.2013, 299 m, J.P. Zaballos & S. Pérez-González leg. (Coll. J.P. Zaballos and Coll. S. Pérez-González, UCM), 5 ♂♂ (BMNH-1046127, BMNH-1046128, BMNH-1046285, BMNH-1046286, BMNH-1046126), 5 ♀♀ (BMNH-1046129, BMNH-1046287, BMNH-1046130, BMNH-1046288, BMNH-1046289), same data (Coll. C. Andújar, NHM, Coll. J.P. Zaballos and Coll. S. Pérez-González, UCM). — DNA aliquots deposited in NHM, London (voucher nº BMNH-1046290, BMNH-1046291, BMNH-1046131, BMNH-1046132, BMNH-1046133, BMNH-1046292, BMNH-1046134, BMNH-1046135, BMNH-1046136, BMNH-1046137, BMNH-1046127, BMNH-1046128, BMNH-1046285, BMNH-1046286, BMNH-1046126, BMNH-1046129, BMNH-1046287, BMNH-1046130, BMNH-1046288 and BMNH-1046289).

Diagnosis. Small endogean Anillini, anophtalmous, with subparallel body covered by microreticulated integument and scattered pubescence, recognizable by the following combination of characters: Vertex with *pars stridens*. Right mandible with two teeth. Subsquare pronotum, with two or three low posterolateral denticles. Elytra with smoothly rounded apical region, lacking denticles. Transverse scutellar organ variable: curved or subtriangular. Variable pattern of umbilicate series: 4+2 or 4+3. Last ventrite with belt, posterior margin smooth and continuous, without lateral notches, pattern of chaetotaxy **l-(s)-s-s-l-s-s/m-s-l-s-s-(s)-l**. Male genitalia: Falciform aedeagus, "rod-shaped" endophallic sclerites, with a curved lateral projection pointing upwards. Ring sclerite with a characteristic "spoon-shaped" distal projection. Female genitalia: stout tubular gonocoxites, without lateral setae; ovoid or subsphaeric spermatheca (Figs. 5, 8A,B).

Description. Length 1.11 – 1.32 mm (males), 1.25 – 1.40 mm (females). Anophthalmous, depigmented, with pubescent and microreticulated integument, ranging from yellowish to brown (Fig. 5). ***Head*** (Fig. 5): approximately as wide (0.23 – 0.30 mm) as long (0.23 – 0.30 mm), covered by subhexagonal microreticulation. Stridulatory organ (*pars stridens*) present in vertex region in both sexes. Posterolateral semilunar notch at both sides of cephalic capsule. Labrum subquadrate or slightly rounded, with thicker cuticle in a triangular region with a middle button. Clypeus with straight anterior margin. Moniliform antennae with 11 antennomeres, progressively more square-shaped towards distal (**morph 1**), the last one pyriform. Stem of 3rd antennomere not elongated. *Sensilla coeloconica* (**sc**) on last antennomere arranged in a pattern of 3 anterodorsal and 1 posterodorsal **sc**. 1 ventral **sc** on antennomeres 5 and 6. Right mandible with two terebral teeth, left mandible without teeth, but with a smooth edge. Labium without special features for the genus, with a blunt middle tooth. Long paraglossae, middle lobe of ligula curved and prominent (shorter than paraglossae). Wide gula, approximately twice as long as

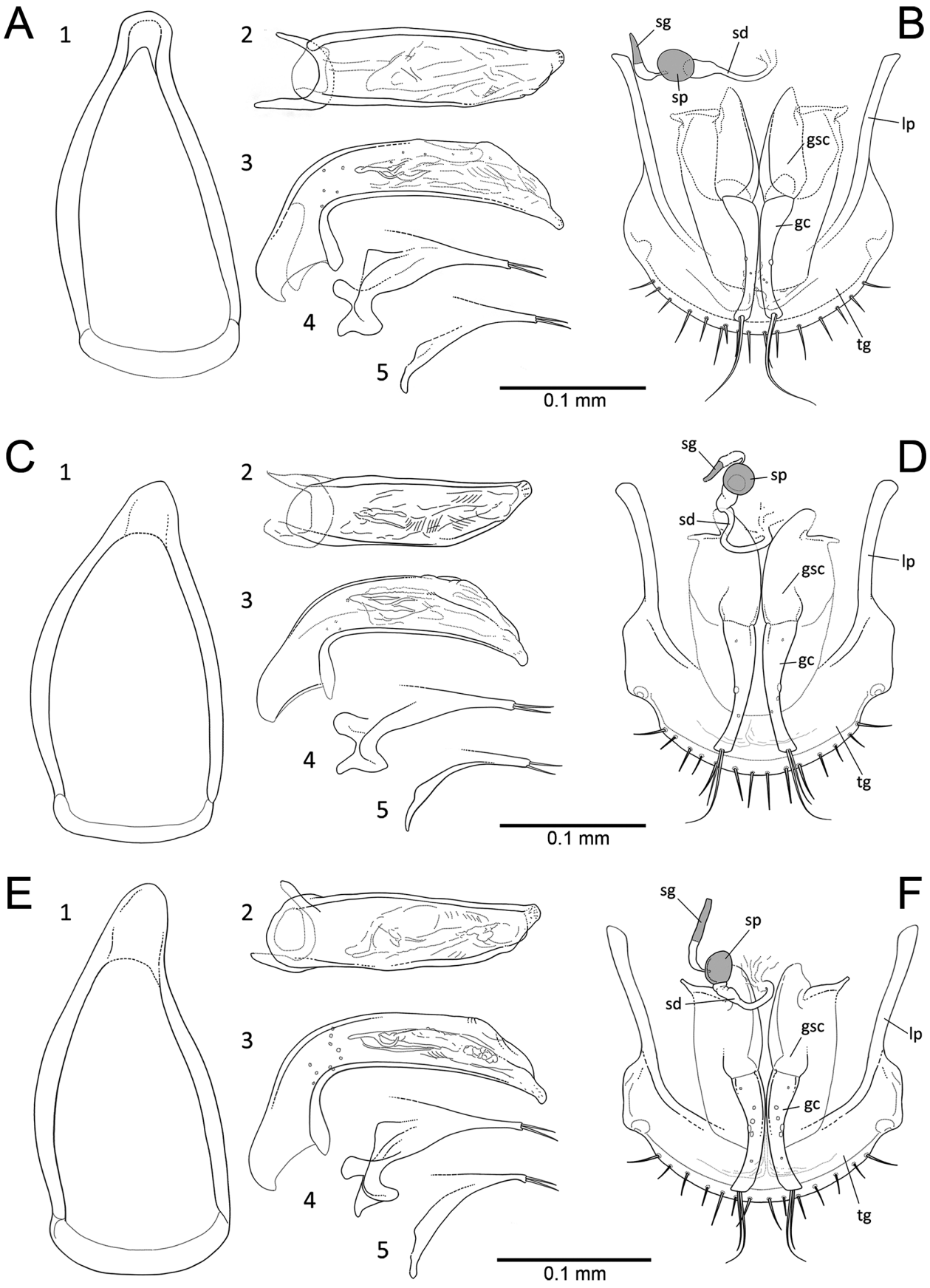

Fig. 8. Genitalia of the three new *Typhlocharis* species. **A**,**B**: *T. coenobita* sp.n. **C**,**D**: *T. eremita* sp.n. **E**,**F**: *T. anachoreta* sp.n. **A**,**C**,**E**: male genitalia: 1: ring sclerite, 2: aedeagus (dorsal view), 3: aedeagus (lateral view), 4: right paramere, 5: left paramere. **B**,**D**,**F**: female genitalia. — ***Abbreviations***: gc – gonocoxite, gsc – gonosubcoxite, lp – lateral projection, sd – spermathecal duct, sg – spermathecal gland, sp – spermatheca, tg – tergite VIII.

wide. *Cephalic chaetotaxy*: 6 pairs of labral setae (**s-s-l-m-s-m/m-s-m-l-s-s**), 2 pairs of clypeal setae (**l-s/s-l**), 1 pair of frontal setae, 2 supraocular pairs (anterior and posterior), 1 supraantenal pair, 2 pairs of occipital setae and 1 pair of genal setae, as well as scattered pubescence. Labium with 1 pair of setae near base of middle tooth, 1 pair of long setae near base of epilobes, 1 pair of very short setae near apex of epilobes and 1 or 2 pairs of very short setae near posterior suture. Prebasilar with 1 pair of lateral setae near anterior margin, 1 pair of very short lateral setae in middle region and 2 pairs (the lateral one much longer) in posterior region, irregularly distributed among specimens. ***Thorax*** (Fig. 5): pronotum subquadrate, barely longer (0.28–0.36 mm) than wide (0.28–0.34 mm), slightly narrowed posteriorly. Anterior margin straight or smoothly curved inwards, slightly crenulated, with medial hiatus (approximately as wide as 2 adjacent intersetal spaces). Posterior margin smoothly sinuated. Lateral margins with 2 or 3 posterior denticles, low, blunt and irregular. Surface covered by subhexagonal microreticulation. Disc flattened, with a medial line and a pair of faint lateral sulci. Chaetotaxy: 1 pair of long setae in anterior third of lateral margins, 1 pair of long setae in posterior angles, a row of 6–8 pairs of setae [**l-(l)-(m)-l-m-l-m-l/l-m-l-m-l-(m)-(l)-l**] parallel to anterior margin (in general, 2 or 3 of them are notably shorter than the rest, alternated with long setae and highly variable among specimens), 3 pairs of setae parallel to posterior margin [**s-l-l/l-l-s**], a row of small, thin setae, regularly placed along anterior and posterior margins, a row of short setae along lateral margins and 5 pairs of irregular longitudinal rows on disc. Proepisternal suture visible. Prosternal apophysis rounded. Anterior margin of prosternum with a row of long and thin setae and 6–8 pairs of short setae parallel to them. Prosternum covered by scattered pubescence, absent in proepisterna. Mesoepisterna barely sunk. Metaepisterna with a pair of smooth lateral foveae, moderately sunk in both sexes. ***Elytra*** (Fig. 5): subparallel, more than twice longer (0.60–0.74 mm) than wide (0.30–0.38 mm). Lateral margins serrated, with 17–22 faint denticles progressively less marked towards posterior. Apical margin round, without denticles, the middle suture ends in a smooth "v-shaped" notch in some specimens. Humeral angle well marked. Disc flattened, with longitudinal carinae associated to 7th stria not reaching apical region. Surface covered in subhexagonal-irregular microreticulation. Elytral pits small and faint, barely visible but scattered along 7th stria and disc. Transverse scutellar organ with curved or subtriangular posterior margin. One pair of slot-shaped "buttonholes" (frequently double), near base of elytra. Chaetotaxy: umbilicate series formed by an anterior group of four setae and a posterior group of 2 (**4+2**) or 3 setae (**4+3**, in the population of Río Guadajira). 1 pair of scutellar setae. No discal setae. 5 or 6 pairs of longitudinal rows of short discal pubescence, slightly longer towards posterior. Apical row of thin setae, apical pair barely longer than the rest. Lateral margins with a short seta for every denticle. ***Legs*** (Fig. 5): similar in both sexes. Profemora, protibiae, mesofemora and mesotibiae without special features. Metacoxal flap smoothly rounded. Metatrochanters rounded. Metafemora slightly angular, thinner proximally. Metatibiae dilated at distal end. Inner side of profemora coarse or smooth, smooth in meso- and metafemora. Tarsi clearly pentamerous in all limbs. Pretarsal claws curved and smooth. ***Abdomen*** (Fig. 5B): covered by irregular microsculpture. Intermetacoxal space not widened. 1st ventrite without ventral foveae. Last ventrite with belt of scaly and thin microsculpture (margin of each scale finely and irregularly serrated in both sexes). Posterior margin smoothly curved, with 6 or 7 pairs of setae without significant sexual dimorphism: **l-(s)-s-s-l-s-s/m-s-l-s-s-(s)-l**. ***Male genitalia*** (Fig. 8A): Aedeagus with falciform median lobe (length 0.21 mm), slightly bent to the right in dorsal view (anatomically oriented). Subtriangular, blunt apex. Endophallus with rod-shaped, forked sclerites, with a curved lateral projection pointing upwards. Subtriangular parameres, with 2 mid-sized apical setae. Ring sclerite (IXth abdominal sternum) subtriangular-arcuate, projected apically in a rounded, broad, "spoon-shaped" expansion. ***Female genitalia*** (Fig. 8B): Stout tubular gonocoxites, with 2 apical setae, according to the general model described by Vigna-Taglianti (1972), without lateral setae but scattered pores. Gonosubcoxites smoothly rounded. Spermathecal duct short to medium length, with two well-differentiated regions: proximal, thinner (diameter 0.003 mm) and distal, thicker (diameter 0.011 mm). Subsphaeric to slightly ovoid spermatheca (length 0.025 mm). Spermathecal gland conical (length 0.021 mm), distally sclerotized. Genital armature (abdominal segment/tergite VIII) with margin smooth and round, covered in a row of thin setae; lateral projections long and thin.

Derivatio nominis. The specific epithet refers to the apparent isolation from the outside world where these animals spent their lives, in homage to the spiritual retirement of the cenobitic monks (from latin *coenobita* as member of a *coenobium*, a group of monks living in isolated communities).

Habitat. This species was collected in four localities within a range of approximately 1000 km² (Fig. 2). In the type locality, Valverde de Burguillos (Fig. 1C), *Typhlocharis coenobita* sp.n. was captured in soil samples from a small meadow surrounded by cultures and open holm oak forest (*Quercus ilex* L.), where it coexists with *T. mixta*. In Valverde de Leganés (Fig. 1D), the sample was taken in reddish to dark brown soil with small embedded boulders from an olive tree culture (*Olea europaea* L.), with dense patches of brooms (*Retama* sp. Raf.) over grasses and thistles, with some holm oaks dispersed (*Quercus ilex* L.). The population of La Albuera (Fig. 1E) was found in a land used for pasture, on a low slope under holm oaks (*Quercus ilex* L.), near a small river surrounded by ash trees (*Fraxinus* sp. Tourn. ex. L.). The locality of Río Guadajira (Fig. 1F) was an open area with reddish, clayish soil and abundant scattered boulders and stones of diverse sizes. Vegetation was composed mainly by

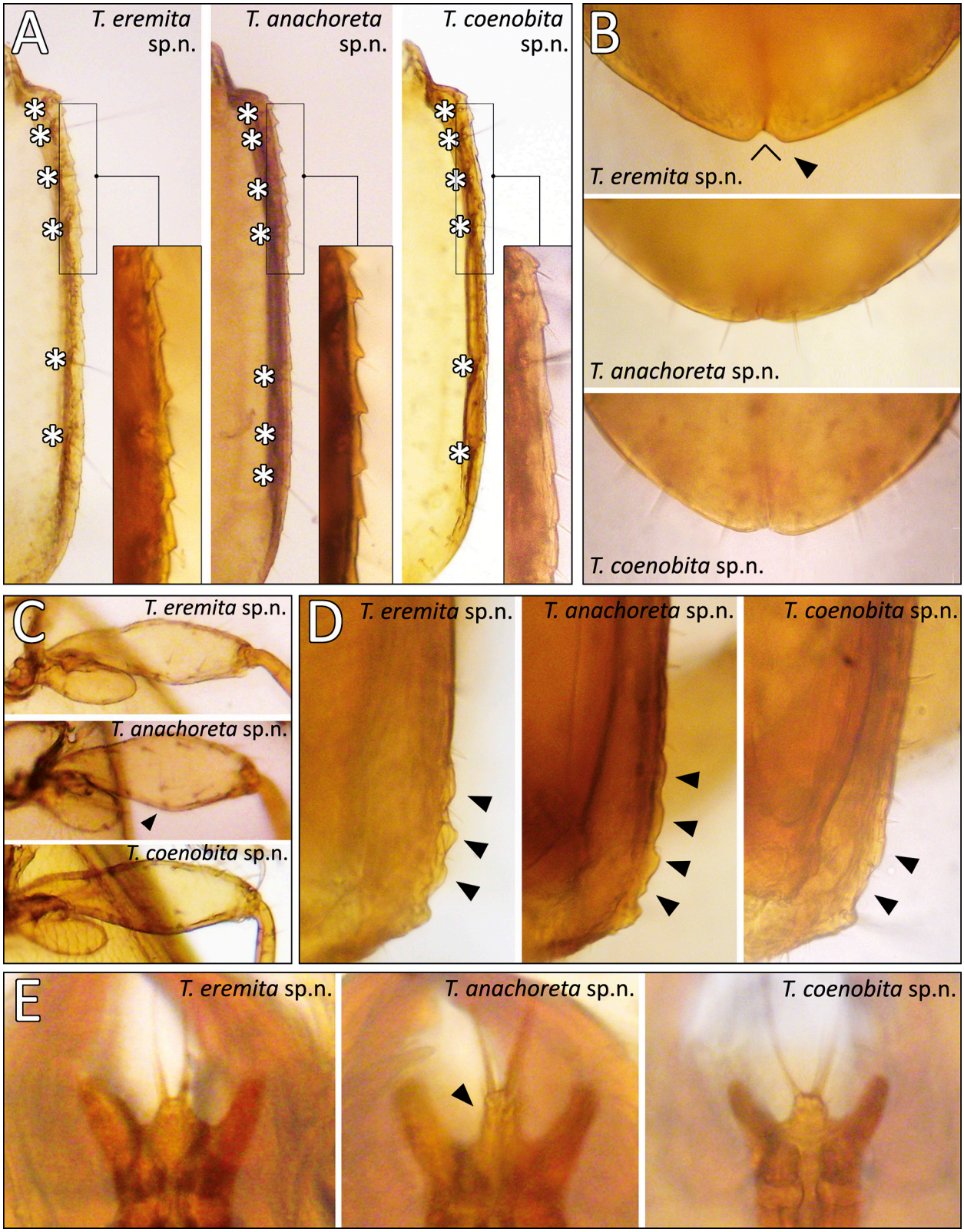

Fig. 9. Comparative detail photographs of the six main discriminant characters in the recognition of the three new *Typhlocharis* species. **A**: pattern of umbilicate series (position of setae indicated by "*") and lateral denticles of elytra. **B**: shape of elytral apex; note the "v-shaped" notch of *T. eremita* sp.n. **C**: shape of metafemora. **D**: posterolateral denticles of pronotum (indicated by black arrows). **E**: median lobe of ligula; note the specially prominent lobe of *T. anachoreta* sp.n.

grasses, thistles and small bushes. The sample was taken from the soil under a large deeply buried boulder, in the unaltered boundaries of a recently ploughed culture.

Variability. The description above is based on the specimens from Valverde de Burguillos, but the other populations show a notable range of variation (Table 1).

Within Valverde de Burguillos (372 specimens), the shape of labrum, development of the terebral teeth (the second tooth can be very blunt in some specimens), shape of the pronotum (specially the anterior margin), width of the hiatus, number and shape of the posterolateral denticles in pronotum, shape of the transverse scutellar organ, shape of the elytral buttonholes, shape of the apex of the elytra or texture of the inner margin of femora are all structures that can express minor differences among individuals. In three specimens the umbilicate series is asymmetric, with a 3+2/4+2 pattern.

The specimens from La Albuera (38 specimens) and Valverde de Leganés (3 specimens) are nearly identical to each other and fall within the range of variation observed in the *T. coenobita* sp.n. from Valverde de Burguillos. However, in average, these populations vary from the specimens in Valverde de Burguillos in a more prominent median lobe of ligula, fainter lateral denticles of elytra, less angular metafemora and smooth inner margin of femora in all limbs (Table 1). The "spoon-shaped" projection in the ring sclerite of males is more heterogeneous. The rest of cephalic features, pronotum, elytra, abdomen and genitalia are coincident.

The specimens from Río Guadajira (56 specimens) are the most morphologically divergent to the other populations (Table 1), with differences that mainly affect pronotum and elytra. In average, they show a wider medial hiatus and generally more sinuous anterior margin (instead of straight) as well as more pronounced posterolateral denticles. The transverse scutellar organ is subtriangular in the majority of specimens (this is the population with stronger development and less variation in this trait). The most conspicuous difference is the pattern of the umbilicate series, 4+3 instead of 4+2 as in the other populations. Ligula, lateral denticles of elytra, inner margin of femora and male genitalia vary in the same degree as the populations of La Albuera and Valverde de Leganés, but the metafemora are angular (as in the specimens from Valverde de Burguillos). Intrapopulation variability is in the same degree and affects the same structures as described for the other populations.

Typhlocharis eremita sp.n.

Locus typicus. Oliva de la Frontera, Badajoz, España.

Material examined. ***Type series***: Holotype: 1 ♂ (BMNH-1046145) SPAIN, Badajoz, Oliva de la Frontera (2.8 km N), Arroyo Zaos (38°17′N 06°54′W), 3.xii.2013, 364 m, J.P. Zaballos & S.Pérez-González leg. (Coll. J.P. Zaballos, UCM). – Paratypes: 1 ♂, 6 ♀♀ same data as the holotype (Coll. J.P. Zaballos and Coll. S. Pérez-González, UCM), 3 ♂♂ (BMNH-1046146, BMNH-1046147, BMNH-1046296), 4 ♀♀ (BMNH-1046143, BMNH-1046144, BMNH-1046297, BMNH-1046298) same data as the holotype (Coll. C. Andújar, NHM, Coll. J.P. Zaballos and Coll. S. Pérez-González, UCM). — DNA aliquots deposited in NHM, London (voucher nº BMNH-1046145, BMNH-1046146, BMNH-1046147, BMNH-1046296, BMNH-1046143, BMNH-1046144, BMNH-1046297 and BMNH-1046298).

Diagnosis. Small endogean Anillini, anophtalmous, with subparallel body covered by microreticulated integument and scattered pubescence, recognizable by the following combination of characters: Vertex with *pars stridens*. Right mandible with two teeth. Subsquare or subrectangular pronotum, with three to five strong posterolateral denticles. Elytra with smoothly rounded apical region, lacking denticles but with a clear "v-shaped" notch. Transverse scutellar organ variable: straight or slightly subtriangular. Umbilicate series with six setae (4+2). Last ventrite with belt, posterior margin smooth and continuous, without lateral notches, pattern of chaetotaxy **l-(s)-s-s-l-s-s/m-s-l-s-s-(s)-l**. Male genitalia: Falciform aedeagus, "rod-shaped" endophallic sclerites, arranged in a branched structure. Ring sclerite with a broad subtriangular distal projection. Female genitalia: tubular gonocoxites, without lateral setae; subsphaeric spermatheca (Figs. 6, 8C,D).

Description. Length 1.26–1.29 mm (males), 1.25–1.43 mm (females). Anophthalmous, depigmented, with pubescent and microreticulated integument, ranging from yellowish to brown (Fig. 6). ***Head*** (Fig. 6): almost as long (0.25–0.30 mm) as wide (0.26–0.30 mm). Cephalic features as described for *T. coenobita* sp.n., with exception of semilunar notches, much less marked, and a generally rounder, smoother labrum. Middle lobe of ligula moderately prominent, curved. *Cephalic chaetotaxy*: follows the same pattern as in *T. coenobita* sp.n. ***Thorax*** (Fig. 6): pronotum: subquadrate to subrectangular, trend to longer (0.31–0.40 mm) than wide (0.30– 0.34 mm) shapes, slightly narrowed in posterior region. Anterior margin straight, crenulated, with medial hiatus as wide as 2–3 adjacent intersetal spaces. 3–5 posterolateral denticles, strong and well defined, in form of undulating edge. Other pronotal features and chaetotaxy as described for *T. coenobita* sp.n. Proepisternal suture visible and prosternal apophysis rounded. Prosternum, mesoepisterna and metaepisterna as in *T. coenobita* sp.n. ***Elytra*** (Fig. 6): approximately 2 × longer (0.66– 0.74 mm) than wide (0.33–0.35 mm), subparallel. Lateral margins with 17–27 subtriangular denticles, progressively less marked towards posterior, but still defined near end. Apical margin without denticles, but with two blunt and rounded angles separated by a clear "v-shaped" notch in the end of suture. Transverse scutellar organ substraight or very smoothly subtriangular. Chaetotaxy: umbilicate series with anterior group of 4 setae and posterior group of 2 setae (**4+2**). Discal pubescence very short, even in apical region, distributed in 5 pairs of longitudinal rows. The rest of features do not differ from those described in *T. coenobita* sp.n. ***Legs*** (Fig. 6): As described for *T. coenobita* sp.n., but smooth inner margins in all femora, metafemora less angular and distal end of metatibiae strongly dilated. ***Abdomen*** (Fig. 6B): Abdominal features and chaetotaxy as described for *T. coenobita* sp.n. ***Male genitalia*** (Fig. 8C): Aedeagus with falciform median lobe (length 0.19 mm), slightly bent to the right in dorsal view (anatomically oriented). Subtriangular, smoothly rounded apex. Endophallus formed by several "rod-shaped" sclerites, arranged in a "branched" structure. Subtriangular parameres, with 2 mid-sized apical setae. Ring sclerite (IXth abdominal sternum) with a broad subtriangular

distal expansion. ***Female genitalia*** (Fig. 8D): adjusts to the model of Vigna-Taglianti (1972). Tubular gonocoxites with 2 apical setae. Lateral setae absent, but scattered pores. Gonosubcoxites rounded. Short spermathecal duct, with two differentiated regions: thinner, proximal (diameter: 0.003 mm) and thicker, distal (diameter 0.010 mm). Subsphaeric to slightly ovoid spermatheca, "bulb-shaped" (length 0.021 mm). Conical spermathecal gland (length 0.020 mm), distally sclerotized. Genital armature (abdominal segment/tergite VIII) with margin smooth and round, covered in a row of thin setae; lateral projections long and slender.

Derivatio nominis. This species is dedicated to the hermit way of life (from latin *eremita*), voluntarily retired from the society, as allusion to the evolutionary history of the lineage, isolated from the external world to live in the endogean environment.

Habitat. The species is only known from the type locality, Zaos stream, near Oliva de la Frontera (Fig. 1A). It was captured in a small slope of a temporary watercourse in an alluvial plain between low hills covered with open cork oak (*Quercus suber* L.) forest. The sample was taken near some oleander bushes (*Nerium oleander* L.) and reeds (*Juncus* sp. L.), also from the underside of a deeply buried stone. The soil was humid and dark brown, rich in organic matter.

Variability. The range of variability in the single population known of *T. eremita* sp.n. (15 specimens) affects mainly the labrum, pronotum, transverse scutellar organ, lateral denticles of elytra, elytral buttonholes and chaetotaxy. This variation occurs in a similar fashion to that observed in *T. coenobita* sp.n., showing subtle variations within the observed specimens in shape, development and number of denticles, or position of setae.

Typhlocharis anachoreta sp.n.

Locus typicus. Higuera de Vargas, Badajoz, España.

Material examined. ***Type series***: Holotype: 1 ♂ SPAIN, Badajoz, Higuera de Vargas (3.15 km S) (38°25′N 06°59′W), 3.xii.2013, 358 m, J.P. Zaballos & S.Pérez-González leg. (Coll. J.P. Zaballos, UCM). – Paratypes: 253 ♂♂, 269 ♀♀ same data as the holotype (Coll. J.P. Zaballos and Coll. S. Pérez-González, UCM), 2 ♂♂, 2 ♀♀ same data as the holotype (MNCN), 4 ♂♂ (BMNH-1046139, BMNH-1046293, BMNH-1046138, BMNH-1046140), 4 ♀♀ (BMNH-1046142, BMNH-1046294, BMNH-1046295, BMNH-1046141) same data as the holotype (Coll. C. Andújar, NHM, Coll. J.P. Zaballos and Coll. S. Pérez-González, UCM). — DNA aliquots deposited in NHM, London (voucher nº BMNH-1046139, BMNH-1046293, BMNH-1046138, BMNH-1046140, BMNH-1046142, BMNH-1046294, BMNH-1046295 and BMNH-1046141).

Diagnosis. Small endogean Anillini, anophtalmous, with subparallel body covered by microreticulated integument and scattered pubescence, recognizable by the following combination of characters: Vertex with *pars stridens*. Right mandible with two teeth. Subquadrate pronotum, with three to five blunt posterolateral denticles. Elytra with smoothly rounded apical region, lacking denticles. Transverse scutellar organ hightly variable: straight to strongly subtriangular. Strongly marked lateral denticles. Umbilicate series with seven setae (4+3). Last ventrite with belt, posterior margin smooth and continuous, without lateral notches, pattern of chaetotaxy **l-(s)-s-s-l-s-s/m-s-l-s-s-(s)-l**. Male genitalia: Falciform aedeagus, "rod-shaped" endophallic sclerites, with a curved lateral projection pointing upwards. Ring sclerite with a broad and variable "spoon-shaped" distal projection. Female genitalia: robust tubular gonocoxites, without lateral setae; slightly ovoid or subsphaeric spermatheca (Figs. 7, 8E,F).

Description. Length 1.17 – 1.35 mm (males), 1.30 – 1.45 mm (females). Anophthalmous, depigmented, with pubescent and microreticulated integument, ranging from yellowish to brown (Fig. 7). ***Head*** (Fig. 7): slightly wider (0.26 – 0.29 mm) than long (0.23 – 0.26 mm). Cephalic features as described for *T. coenobita* sp.n., but inner edge of left mandible more prominent and middle lobe of ligula highly projected, as long or longer than paraglossae. *Cephalic chaetotaxy*: coincident with the pattern described in *T. coenobita* sp.n. ***Thorax*** (Fig. 7): pronotum subquadrate, slightly longer (0.32 – 0.40 mm) than wide (0.29 – 0.36 mm) narrowed posteriorly. Anterior margin straight or smoothly curved inwards with medial hiatus as wide as 2 or 3 adjacent intersetal spaces. 3 – 5 posterolateral denticles, blunt and irregular but well defined. Rest of pronotal features and chaetotaxy as described for *T. coenobita* sp.n. Proepisternal suture visible and prosternal apophysis rounded. Prosternum, mesoepisterna and metaepisterna as in *T. coenobita* sp.n. ***Elytra*** (Fig. 7): approximately 2 × longer (0.62 – 0.79 mm) than wide (0.32 – 0.40 mm), subparallel. Lateral margins serrated with 17 – 27 strongly marked denticles, progressively smoother towards posterior, but still defined near end. Apical margin without denticles. Transverse scutellar organ highly variable, margin substraight to strongly subtriangular. Chaetotaxy: umbilicate series formed by anterior group of four setae and posterior group of three setae (**4+3**). Apical row of thin setae, apical pair longer than rest. Other features as described for *T. coenobita* sp.n. ***Legs*** (Fig. 7): As described for *T. coenobita* sp.n., but smooth inner margins in all femora. ***Abdomen*** (Fig. 7B): abdominal features and chaetotaxy as described for *T. coenobita* sp.n. ***Male genitalia*** (Fig. 8E): Aedeagus with falciform median lobe (length: 0.19 mm), slightly bent to the right in dorsal view (anatomically oriented). Subtriangular, smoothly rounded apex. Endophallus with rod-shaped, forked sclerites and a curved lateral projection pointing upwards. Subtriangular parameres, with 2 mid-sized apical setae. Ring sclerite (IXth abdominal sternum) with a broad "spoon-shaped" distal expansion, irregular and highly variable between individuals, more or less square edges are common. ***Female genitalia*** (Fig. 8F): adjusts to the model of Vigna-Taglianti (1972). Robust tubular gonocoxites with 2 apical setae. Lateral setae absent, but scattered pores. Gonosubcoxites rounded.

Short spermathecal duct, with two differentiated regions: thinner, proximal (diameter 0.004 mm) and thicker, distal (diameter 0.008 mm). Slightly ovoid or subsphaeric spermatheca (length 0.022 mm). Conical spermathecal gland (length 0.029 mm), distally sclerotized (Fig. 8F). Genital armature (abdominal segment/tergite VIII) with margin smooth and round, covered in a row of thin setae; lateral projections long and slender.

Derivatio nominis. Like the cenobitic monks or the hermits, the anchorites (from latin *anachoreta*) were people retired from the society to a life of isolation. The new species is named after them by the parallel lifestyle, retired from the outside to a life inside the soil.

Habitat. *T. anachoreta* sp.n. is currently known only from the type locality, near Higuera de Vargas (Fig. 1B), where it was found in an open grassland and thistle pasture field with scattered broom bushes (*Retama* sp. Raf.). Abundant small boulders and stones were scattered all over the place, embedded in the soil at general shallow depths (5–20 cm). The sample was taken from humid soil under the stones.

Variability. The morphological traits that are observed to vary between individuals of *T. anachoreta* sp.n. are the same as commented before in *T. coenobita* sp.n. and *T. eremita* sp.n. Apart from that, the population of Higuera de Vargas is quite diverse in size and degree of sclerotization, from soft, yellowish small specimens around 1.15 mm to tougher, chestnut brown large specimens of more than 1.40 mm.

3.4. Identification key to the "*coenobita* species complex"

1 Presence of ventral foveae on 1st ventrite, more developed in females. Inner margin of profemora markedly angular .... ***T. mendesi* Serrano & Aguiar 2017**

1' Absence of ventral foveae. Inner margin of profemora not or smoothly angular **2**

2 Faint semilunar notch. Posterolateral denticles of pronotum strong and well defined, 3–5 (Fig. 9D). "v-shaped" notch in the elytral apex (Fig. 9B). Subtriangular distal expansion of ring sclerite (Fig. 8C) ..... ***T. eremita* sp.n.**

2' Well marked semilunar notch. Moderately marked or low posterolateral denticles of pronotum (Fig. 9D). Elytral apex rounded, without any clear "v-shaped" notch (Fig. 9B). "Spoon-shaped" distal expansion of ring sclerite (Fig. 8A,E) **3**

3 Very prominent middle lobe of ligula (as long as or longer than paraglossae, Fig. 9E). Posterolateral denticles of pronotum moderately marked, 3–5 (Fig. 9D). Lateral denticles of elytra strongly marked, serrated (Fig. 9A) ..... ***T. anachoreta* sp.n.**

3' Curved middle lobe of ligula, sometimes prominent, always shorter than paraglossae. Posterolateral denticles of pronotum low and blunt, 2–4. Lateral denticles of elytra faint or very faint ... ***T. coenobita* sp.n.**

4. Discussion

4.1. Affinities

Typhlocharis coenobita, *T. eremita* and *T. anachoreta*, hence referred as the "*coenobita* complex", are very close to each other and represent a lineage previously unknown for the genus (Pérez-González et al. 2017). This lineage was shown related to species of the former "*baetica*" group (except *T. mixta*) and *T. besucheti*, *T. martini*, *T. singularis* and *T. gomesalvesi*.

T. eremita is easily distinguished within the complex by a fainter semilunar notch, pronotum with well marked crenulation in the anterior margin and 3–5 strong, well defined posterolateral denticles, elytra with moderately marked lateral denticles and a characteristic "v-shaped" notch in the apex (Fig. 9, Table 1). Also, it is recognizable by some features of male genitalia, like the shape of endophallic scleries and the distal expansion of the ring sclerite.

T. coenobita shows high internal variability between populations and it is the second described species of Typhlocharina with a polymorphic pattern of umbilicate series (Serrano & Aguiar 2000, 2002). Morphological features of the RG population are beyond the average variation observed for the other populations of *T. coenobita*. Some characteristics of the RG specimens (like the 4+3 umbilicate series, the prominent middle lobe of ligula, the width of the medial hiatus among others, see Table 1) are close to that of *T. anachoreta*. This fills a morphological gradient that challenges the differentiation between *T. coenobita* and *T. anachoreta*. However, *T. anachoreta* can be identified by the extremely prominent middle lobe of the ligula, the posterolateral denticles of pronotum (more abundant and notorious than in *T. coenobita*) and the strongly marked lateral denticles of elytra (Fig. 9), much more developed than in any population of *T. coenobita*.

The combination of a reduced pattern in the umbilicate series (4+2, 4+3) and total lack of apical denticles in elytra is unusual within Typhlocharina. So far, this condition was only known in *T. armata* Coiffait, 1969; *T. deferreri* Zaballos & Pérez-González, 2011 and the recently described *T. mendesi* (Zaballos & Pérez-González 2011a,b; Serrano & Aguiar 2017). *T. armata* and *T. deferreri* are distantly related to the "*coenobita* complex" (Pérez-González et al. 2017) and, while the overall morphology is similar, they do not share characteristic traits of the complex, such as the alternate length in the setae of anterior margin of pronotum, the shape of the ring sclerite of males or the short spermathecal duct and rounded spermathecae of females. By contrast, *T. mendesi* show all these features, suggesting that it is a member of the same species complex. We had the oppor-

tunity of studying four paratypes of *T. mendesi* (2 males, 2 females) that indicates a particularly close relationship to *T. eremita*. Both species share a trend to rectangular pronotums with well marked crenulation in the anterior margin and moderately marked lateral denticles of elytra, as well as a near-identical shape of the ring sclerite projection. *T. mendesi* differs from the three new species in the presence of well developed ventral foveae in the first ventrites (deeper in females) and very angular profemora. The fact that *T. mendesi* is only known from the surroundings of Bucelas region (Estremadura, Portugal), about 200 km away from the area where the new species were found (southern Badajoz, Spain) points to a wider distribution of the *coenobita* species complex.

The subtriangular shape of the transverse scutellar organ, the pattern of the endophallic sclerites and the shape of the spermatheca resemble those of *T. martini* Andújar, Lencina & Serrano, 2008; *T. besucheti* Vigna-Taglianti, 1972; *T. gomesalvesi* Serrano & Aguiar, 2002 and *T. singularis* Serrano & Aguiar, 2000, which are characterized by the presence of parasutural denticles in the elytral apex. *T. gomesalvesi* and *T. singularis* are the closest geographically, and also show reduced umbilicate series (4+2), polymorphic in the case of *T. singularis* (Serrano & Aguiar 2000, 2002).

The pattern of the endophallic sclerites, with bifurcated rod-shaped pieces and a lateral branch pointing upwards, is also typical of the *baetica* group (Pérez-González & Zaballos 2013a). This is suggestive of a relationship between all the mentioned species that is supported in the current phylogenies of Typhlocharina (Pérez-González et al. 2017; Andújar et al. 2017). In fact, the main difference between "*coenobita* complex", *T. martini*, *T. besucheti*, *T. gomesalvesi*, *T. singularis* and the species of *baetica* group is the different development of apical denticles in the elytra (absent, presence of microdenticles and sutural denticles and multiple fully developed denticles, respectively), which have been shown to be plastic characters with low phylogenetic signal (Pérez-González et al. 2017).

4.2. Lumping or splitting? Taxonomic implications of the new populations

While the reality of the species concept as discrete entities and the boundaries of speciation processes has been thoroughly discussed (e.g. De Queiroz 2007; Willis 2017; Sites & Marshall 2003), the designation of evolutionary lineages is still a need that should be attained to register and describe biological diversity (Dayrat 2005; Valdecasas 2008).

The three species proposed in this work are supported by morphological and molecular data and all of them differ from any other *Typhlocharis* species. The entity of *T. eremita* as a new species is well established within the standards of the genus. However, the high internal variability observed within the populations of *T. coenobita* and their relationship with *T. anachoreta* are in the verge of what can be considered species-level differentiation. In particular, the population of Río Guadajira implies an interesting problem. Morphologically, this population shows some features that are intermediate between other populations of *T. coenobita* and *T. anachoreta*, blurring the otherwise clear differences between the two taxa (Table 1). In addition, all populations within *T. coenobita* do not share haplotypes and show certain geographic structure (Fig. 2). This situation led to discuss different taxonomic interpretations:

Why not consider RG as a different species? According to the mitochondrial sequences studied, the populations described as *T. coenobita* show heterogeneity, pointing to a certain level of isolation between three large clusters (VL+LA, VB and RG respectively). The current molecular phylogeny suggests that RG population is nested within the same clade as the remaining populations of *T. coenobita*, with a sister relationship with specimens from VB (Fig. 3B). Thus, describing the RG population as a different species would imply that the other two lineages should be at the same taxonomic level, i.e. *T. coenobita* would be split into three different taxa (RG, VB and VL+LA). The subtle morphological differences between the populations of VB and VL+LA do not support their division in two species, while describing specimens from VB and VL+LA as a single species, excluding RG, would generate an artificial, paraphyletic taxon.

Does the RG population fall within the internal variability of *T. coenobita*? According to the statistical analyses, yes. It is possible to accurately discriminate between the three new species with a 100% rate of success based on six morphological key characters in agreement with the results of the discriminant analyses.

This classification was tested with the additionally coded specimens and the RG specimens were recognized as *T. coenobita* in all cases. This implies that the RG population is, overall, closer to the rest of *T. coenobita* in spite of the aforementioned affinities with *T. anachoreta*. The use of statistical analysis in taxonomy and integrative studies with molecular and morphological data is becoming more and more common (e.g. Silva et al. 2017), yet this is the first time that such techniques are applied to discriminate species in Anillini endogean beetles. They suppose a powerful tool that could help taxonomic decisions when phenotypic differences are difficult to assess.

Why not consider *T. anachoreta* as part of *T. coenobita*? In this case, the molecular data (Fig. 3B) recovered a well supported relationship of the population from HV, described as *T. anachoreta*, as the sister taxon to the whole clade of *T. coenobita* populations. Molecular data indicates a higher separation between both clades than within any of the populations of *T. coenobita*.

Also, the morphological differences between both clades go beyond the usual limits of internal variability known in *Typhlocharis* (Pérez-González et al. 2013).

Wiens & Servedio (2000) pointed to the need of many individuals to assess that a diagnostic character is fixed in a species. *T. coenobita* and *T. anachoreta* fill this requirement and, with a sample of 469 and 535 specimens respectively, the differences between lateral denticles of elytra and the prominence of the middle lobe of ligula are consistent (Fig. 9). Lumping *T. anachoreta* as a part of *T. coenobita* would be unpractical, given the difficulty to provide an efficient diagnosis for the species.

Overall, although different taxonomic decisions are possible, we consider that the species boundaries here adopted maximize the consistence among different sources of evidence data, while the intraspecific variability within *T. coenobita* is properly described and discussed, thus contributing to elucidate the ongoing differentiation processes within the *coenobita* species complex.

4.3. Evolutionary remarks

The "*coenobita* species complex" is the first documented case of an expected situation within Typhlocharina and other lineages of Anillini: the presence of several closely related allopatric populations within a very reduced geographical range that, despite certain genetic isolation, show a gradient of morphological differences that challenge their taxonomic assignment. This pattern of strong phylogeographic structure at a reduced spatial scale has been also documented in other edaphic arthropods (e.g. Emerson et al. 2011; Andújar et al. 2015; Faille et al. 2015; Bennet et al. 2016; von Saltzwedel et al. 2016).

It has been stated that these animals use passive waterborne dispersal mechanisms as well as short-distance active displacement of the populations (Ortuño & Gilgado 2011; Andújar et al. 2017). The studied populations show a geographic structure (Fig. 2) that could be consistent with two alternative scenarios. In the first one, sporadic dispersal events (active or passive) will allow colonization of new suitable patches of habitat in the surroundings where, due to i) founder effects and ii) subsequent low connectivity between the ancestral and the new populations, differentiation can be achieved in short evolutionary time. In this scenario, the different degrees of variation between the populations of the "*coenobita* species complex" would be due to the different times since the split of populations.

According to the calibrated phylogeny by Andújar et al. (2017), the split of the "*coenobita* species complex" from other *Typhlocharis* could be dated back to about 20 Mya. This provides enough time to make probable infrequent events of dispersal through unsuitable habitats, but also it is enough time for strong environmental changes to happen. Thus, as a second alternative scenario, the data can be coherent with the fragmentation of an ancestral species with a wider distribution and the subsequent isolation and differentiation of resultant populations.

In both scenarios, the differences between the populations of *T. coenobita* are suggestive of incipient speciation processes, where they are in different stages of isolation and show polymorphic characters fixed differently between them. This happens with the different pattern of umbilicate series in RG (4+3) and VL, LA and VB (4+2), which among other differences might be evidence towards future species-level differentiation. As well, *T. coenobita* + *T. anachoreta*, estimated to have split about 5 Mya, could be considered a "macrospecies" (*sensu* Brooks & McLennan 2002), where both lineages have recently diverged.

There is increasing evidence that similar situations could be frequent within the whole lineage of Typhlocharina (Serrano & Aguiar 2000, 2002, 2014; Pérez-González et al. 2013, Pérez-González et al. 2017). This is not surprising considering the great bias derived from the difficulties in the sampling of these minute beetles, where we only get small glances of the real diversity of the lineage. The presence of *T. mendesi* far away of the distributional core of the three new species, strongly suggest this species complex could be far more extended and further data is needed to comprehend the evolutionary history of these minute Iberian endemisms.

5. Acknowledgements

We thank Dr. Paloma de las Heras and Dr. Abel Sanchez for the help and advice with the statistical analyses performed in this work; Dr. Artur Serrano, for the kind donation of four specimens of *T. mendesi* that allowed direct comparison of this species with the studied populations; Dr. Carmen Callejas, Dr. Paula Arribas and Dr. Jacinto Berzosa provided valuable comments and support during the elaboration of the manuscript. Dr. Alfried Vogler contributed to fund the generation of molecular data. This research has been partially funded by projects CGL2010-16944 (Spanish Ministry of Education) and GR35/10-A Research Group 921632 (Santander-UCM). S.P.G. received support from a postdoctoral Juvenile Employment grant (CT53/16-CT54/16) at the Universidad Complutense de Madrid and C.A. from a Marie Curie postdoctoral grant (Project SOILBIODIV-705639; Program H2020-MSCA-IF-2015).

6. References

Andújar C., Arribas P., Ruiz C., Serrano J., Gómez-Zurita J. 2014. Integration of conflict into integrative taxonomy: fitting hybridization in species delimitation of *Mesocarabus* (Coleoptera: Carabidae). – Molecular Ecology **23**: 4344–4361. doi: 10.1111/mec.12793

Andújar C., Arribas P., Ruzicka F., Crampton-Platt A., Timmermans M.J., Vogler A.P. 2015. Phylogenetic community ecology of soil biodiversity using mitochondrial metagenomics. – Molecular Ecology **24**: 3603–3617.

Andújar C., Faille A., Pérez-González S., Zaballos J.P., Vogler A.P., Ribera I. 2016. Gondwanian relicts and oceanic dispersal in a cosmopolitan radiation of euedaphic ground beetles. – Molecular Phylogenetics and Evolution **99**: 235–246.

Andújar C., Pérez-González S., Arribas P., Zaballos J.P., Vogler A.P., Ribera I. 2017. Speciation below ground: Tempo and mode of diversification in a radiation of endogean ground beetles. – Molecular Ecology **26**: 6053–6070. https://doi.org/10.1111/mec.14358

Bameul F. 1990. Le DMHF: un excellent milieu de montage en entomologie. – L'Entomologiste **46**: 233–239.

Bennet K.R., Hogg I.D., Adams B.J., Herbert P.D.N. 2016. High levels of intraspecific genetic divergences revealed for Antarctic springtails: Evidence for small-scale isolation during Pleistocene glaciations. – Biological Journal of the Linnean Society **119**: 166–178.

Berlese A. 1905. Apparachio per raccogliere presto ed in gran numero piccolo Artropodi. – Redia **2**: 85–89.

Brooks D.R., McLennan D.A. 2002. The Nature of Diversity. – Chicago University Press, Chicago. 676 pp.

Clement M., Posada D., Crandall K. 2000. TCS: a computer program to estimate gene genealogies. – Molecular Ecology **9**: 1657–1660.

Coyne J.A., Orr H.A. 2004. Speciation. – Sinauer Associates, Sunderland, Massachusetts. 545 pp.

Dayrat B. 2005. Towards integrative taxonomy. – Biological Journal of the Linnean Society **85**: 407–415.

De Queiroz K. 2007. Species concepts and species delimitation. – Systematic Biology **56**: 879–886.

Emerson B.C., Cicconardi F., Fanciulli P.P., Shaw P.J.A. 2011. Phylogeny, phylogeography, phylobetadiversity and the molecular analysis of biological communities. – Philosophical Transactions of the Royal Society of London, Series B, Biological Sciences **366**: 2391–2402.

Excoffier L., Lischer H.E.L. 2010. Arlequin suite ver 3.5: a new series of programs to perform population genetics analyses under Linux and Windows. – Molecular Ecology Resources **10**: 564–567.

Faille A., Tänzler R., Toussaint E.F.A. 2015. On the way to speciation: shedding light on the karstic phylogeography of the microendemic cave beetle *Aphaenops cerberus* in the Pyrenees. – Journal of Heredity **106**: 692–699. doi.org/10.1093/jhered/esv078

Futuyma D.J. 1998. Evolutionary Biology. 3rd edn. – Sinauer Associates, Sunderland, Massachusetts.

Jeannel R. 1963. Monographie des Anillini, Bembidiides endogés (Col. Trechidae). – Memories Museum National d'Histoire Naturelle (N.S) Zoologie **28**: 33–204.

Jordan D.S. 1905. The origin of species through isolation. – Science **22**: 545–562.

Kalyaanamoorthy S., Minh B.Q., Wong T.K.F., von Haeseler A., Jermiin L.S. 2017. ModelFinder: fast model selection for accurate phylogenetic estimates. – Nature Methods **14**: 587–589. http://dx.doi.org/10.1038/nmeth.4285

Katoh K., Misawa K., Kuma K., Miyata T. 2002. MAFFT: a novel method for rapid multiple sequence alignment based on fast Fourier transform. – Nucleic Acids Research **30**: 3059–3066.

Kearse M., Moir R., Wilson A., Stones-Havas S., Cheung M., Sturrock S., Buxton S., Cooper A., Markowitz S., Duran C., Thierer T., Ashton B., Mentjies P., Drummond A. 2012. Geneious Basic: an integrated and extendable desktop software platform for the organization and analysis of sequence data. – Bioinformatics **28**: 1647–1649.

Kimura M. 1980. A simple method for estimating evolutionary rates of base substitutions through comparative studies of nucleotide sequences. – Journal of Molecular Evolution **16**: 111–120.

Kisel Y., Barraclough T.G. 2010. Speciation has a spatial scale that depends on levels of gene flow. – The American Naturalist **175**: 316–334.

Lomolino M.V., Riddle B.R., Whittaker R.J., Brown J.H. 2010. Biogeography. 4th edn. – Sinauer Associates, Sunderland, Massachusetts. 878 pp.

Mayr E. 1963. Animal Species and Evolution. – Hardvard University Press, Cambridge. 797 pp.

Minh B.Q., Nguyen M.A.T., von Haeseler A. 2013. Ultrafast approximation for phylogenetic bootstrap. – Molecular Biology and Evolution **30**: 1188–1195. http://dx.doi.org/10.1093/molbev/mst024

Nguyen L.T., Schmidt H.A., von Haeseler A., Minh B.Q. 2015. IQ-TREE: a fast and effective stochastic algorithm for stimating maximum-likelihood phylogenies. – Molecular Biology and Evolution **32**: 268–274. http://dx.doi.org/10.1093/molbev/msu300

Normand H. 1911. Description d'un nouveau procédé de capture de Coléopteres hypogés. – L'Echange **315**: 114–116 & 124–126.

Ortuño V.M. 2000. Nueva especie de *Typhlocharis* Dieck, 1869, de la península Ibérica (Coleoptera, Carabidae, Trechinae). – Bulletin de la Société Entomologique de France **105**: 279–284.

Ortuño V.M., Gilgado J.D. 2011. Historical perspective, new contributions and an enlightening dispersal mechanism for the endogean genus *Typhlocharis* Dieck 1869 (Coleoptera: Carabidae: Trechinae). – Journal of Natural History **45**: 1233–1256.

Pérez-González S., Zaballos J.P. 2012. Re-description of two species of *Typhlocharis* (Coleoptera: Carabidae: Anillini) and revision of the models of female genitalia within the genus. – Zootaxa **3279**: 46–62.

Pérez-González S., Zaballos J.P. 2013b. Antennal morphology of the endogean carabid genus *Typhlocharis* (Coleoptera: Carabidae: Anillini): description of sensilla and taxonomic implications. – Journal of Morphology **274**: 809–823.

Pérez-González S., Zaballos J.P. 2013c. Tarsal tetramery and extreme size reduction in Anillini (Coleoptera, Carabidae, Trechinae): the case of *Typhlocharis* Dieck, 1869; description of three new species and definition of a new intrageneric species group. – Zootaxa **3682**: 249–269.

Pérez-González S., Zaballos J.P., Ghannem S. 2013. Intraspecific variation in *Typhlocharis* Dieck, 1869 (Coleoptera, Carabidae, Anillini): the case of two new species of the *baetica* group. – Zootaxa **3710**: 46–60.

Pérez-González S., Andújar C., Zaballos J.P. 2017. Hidden biodiversity: total evidence phylogenetics and evolution of morphological traits in a highly diverse lineage of endogean ground beetles, *Typhlocharis* Dieck, 1869 (Carabidae, Trechinae, Anillini). – Cladistics doi:10.1111/cla.12208

Rohlf F.J. 2000. NTSYS-pc Numerical taxonomy and multivariate analysis system. Version 2.10 manual. – Applied Biostatistics, Inc., N.Y.

Serrano A.R.M., Aguiar C.A.S. 2000. Description of two new endogean beetle species (Coleoptera; Carabidae) from Portugal. – Boletim da Sociedade Portuguesa de Entomologia **7**: 149–158.

Serrano A.R.M., Aguiar C.A.S. 2002. The genus *Typhlocharis* Dieck, 1869 (Coleoptera, Carabidae) in Portugal: description of two new species and faunistic notes. – Boletim da Sociedade Portuguesa de Entomologia **7**: 181–197.

Serrano A.R.M., Aguiar C.A.S. 2014. The genus *Typhlocharis* Dieck, 1869 (Coleoptera: Carabidae): description of a new species from Portugal and remarks on the external microsculpture of the last abdominal sternum "belt". – Annales de la Société Entomologique de France **50**: 202–212.

Serrano A.R.M., Aguiar C.A.S. 2017. A new species of the genus *Typhlocharis* Dieck, 1869 (Coleoptera, Carabidae) from Portugal. – Revue Suisse de Zoologie **124**: 39–46.

Silva T., Guzmán A., Urantówka A.D., Mackiewicz P. 2017. A new parrot from the Yucatán Península, Mexico – its position within genus *Amazona* based on morphology and molecular phylogeny. – PeerJ 5:e3475; DOI 10.7717/peerj.3475

Sites J.W. Jr., Marshall J.C. 2003. Delimiting species: a Renaissance issue in systematic biology. – Trends in Ecology & Evolution **18**: 462–470.

Sokolov I.M., Kavanaugh D.H. 2014. The *integripennis* species group of *Geocharidius* Jeannel, 1963 (Carabidae, Bembidiini, Anillina) from Nuclear Central America: a taxonomic review with notes about biogeography and speciation. – ZooKeys **443**: 61–118.

Tamura K., Peterson D., Peterson N., Stecher G., Nei M., Kumar S. 2011. MEGA5: molecular evolutionary genetics analysis using maximum likelihood, evolutionary distance, and maximum parsimony methods. – Molecular Biology and Evolution **28**: 2731–2739.

Templeton A.R., Crandall K.A., Sing C.F. 1992. A cladistic analysis of phenotypic associations with haplotypes inferred from restriction endonuclease mapping and DNA sequence data. III. Cladogram estimation. – Genetics **132**: 619–633.

Valdecasas A.G., Williams D., Wheeler Q.D. 2008. 'Integrative taxonomy' then and now: a response to Dayrat (2005). – Biological Journal of the Linnean Society **93**: 211–216.

Vigna-Taglianti A. 1972. Un nuovo *Typhlocharis* di Spagna (Col., Carab.). – Bolletino della Societá Entomologica Italiana **104**: 148–156.

von Saltzwedel H., Scheu S., Schaeffer I. 2016. Founder events and pre-glacial divergences shape the genetic structure of European Collembola species. – BMC Evolutionary Biology **16**: 148. doi: 10.1186/s12862-016-0719-8

Wiens J.W., Servedio M.R. 2000. Species delimitation in systematics: inferring diagnostic differences between species. – Proceedings of the Royal Society of London, Series B **267**: 631–636.

Willis S.C. 2017. One species or four? Yes!... and, no. Or, arbitrary assignment of lineages to species obscures the diversification processes of Neotropical fishes. – PLoS ONE **12**: e0172349. https://doi.org/10.1371/journal.pone.0172349

Zaballos J.P. 2003. Carabidae: Trechinae: Anillini. Pp. 237–241 in: Löbl I., Smetana A. (eds), Catalogue of Palaeartic Coleoptera, Vol. 1. – Stenstrup: Apollo Books.

Zaballos J.P. 2005. Los *Geocharis* Ehlers, 1883 de Marruecos y Cádiz (España) (Coleoptera, Carabidae, Trechinae, Anillini). – Graellsia **61**: 61–81.

Zaballos J.P., Pérez-González S. 2011a. A new species of *Typhlocharis* Dieck, 1869 (Coleoptera: Carabidae: Anillini) from South Spain, with notes on the phylogenetic value of sexually related characters and the presence of stridulatory organ (*pars stridens*) in the genus. – Zootaxa **2786**: 42–50.

Zaballos J.P., Pérez-González S. 2011b. *Typhlocharis* vicariantes del Estrecho de Gibraltar. II: *T. silvanoides* Dieck, 1869 (Coleoptera, Caraboidea, Trechidae). – Graellsia **67**: 135–149.

Zaballos J.P., Ruíz-Tapiador I. 1997. Nuevos *Typhlocharis* Dieck (Coleoptera: Caraboidea: Trechidae) de España. – Graellsia **52**: 95–106.

Zaballos J.P., Wrase D. 1998. Tres nuevos *Typhlocharis* Dieck, 1869 (Coleoptera, Caraboidea, Trechidae) de Navarra (España). – Graellsia **54**: 43–52.

Zaballos J.P., Andújar C., Pérez-González S. 2016. A small carabid for a great entomologist: *Typhlocharis amara*, a new species dedicated to Dr. Fritz Hieke (Coleoptera, Carabidae, Anillini). – Entomologische Blätter und Coleoptera **112**: 465–473.

Electronic Supplement Files

at http://www.senckenberg.de/arthropod-systematics

File 1: perezgonzalez&al-carabidaetyphlocharis-asp2018-electronicsupplement-1.doc — **Appendix S1.** — **Table S1.1.** List of vouchered specimens and Genbank accession numbers. From Pérez-González et al. (2017) and Andújar et al. (2017). — **Table S1.2.** List of characters and character transformation series. Adapted from Pérez-González et al. (2017). — **Table S1.3.** "Specimen-level" matrix of morphological data for the 44 hologenophores. In grey, characters recovered as significant predictor variables in the Discriminant Analysis. — **Table S1.4.** "Population-level" matrix of morphological data. *Species hypothesis used in the Discriminant Analysis: A, B and C equivalent to "*T.* sp. 8"; "*T.* sp. 7" and "*T.* sp. 6" respectively, from Pérez-González et al. (2017). In grey, characters recovered as significant predictor variables in the Discriminant Analysis. — **Table S1.5.** Matrix of morphological data for the 43 additional specimens coded to test the performance of the classification function coefficients obtained by the Discriminant Analysis. Highlighted in red, characters recovered as significant predictor variables.

File 2: perezgonzalez&al-carabidaetyphlocharis-asp2018-electronicsupplement-2.doc—**Appendix S2. UPGMA analysis**.—**Table S2.1.** Distance matrix based on Euclidean coefficient for the 44 vouchered specimens. — **Fig. S2.1.** "Specimen-level" UPGMA dendrogram clustering the 44 vouchered specimens by morphological similarity according to 23 characters. Numbers at each node represent bootstrap values (over 100). — **Table S2.2.** Distance matrix based on Euclidean coefficient for the 6 studied populations. — **Fig. S2.2**. "Population-level" UPGMA dendrogram clustering the 6 studied populations by morphological similarity according to 23 characters. Numbers at each node represent bootstrap values (over 100). — **Appendix S3. Discriminant Analysis.** — **Table S3.1.** Results of applying the Classification Functions obtained by the Discriminant Analysis to the 43 additional specimens coded in Table S5. In grey, characters recovered as significant predictor variables. In red, values of the predicted group for each specimen. — **Appendix S4. AMOVA Analysis**.

Zoobank Registrations

at http://zoobank.org

Present article: http://zoobank.org/urn:lsid:zoobank.org:pub:6356F7BC-BSC2-43BF-AB02-F4381575AS20

***Typhlocharis coenobita* Pérez-González, Andújar, Lantero & Zaballos:** http://zoobank.org/urn:lsid:zoobank.org:act:5A16DEB6-8CCE-44C5-A669-BA487A52BFD5

***Typhlocharis eremita* Pérez-González, Andújar, Lantero & Zaballos:** http://zoobank.org/urn:lsid:zoobank.org:act:D51C7A94-536A-4E0A-BBA9-CD4EF6D0B5CD

***Typhlocharis anachoreta* Pérez-González, Andújar, Lantero & Zaballos:** http://zoobank.org/urn:lsid:zoobank.org:act:D3F14F3B-03DF-40E6-9850-D9448559BB31